Response to Reviewer 1

We would like to thank the reviewer for their time to review our paper. In this response, we have addressed the reviewer's comments by providing clarifications and indicating how we edited the manuscript. The reviewer's comments are copied with a gray background, and our responses are provided with a white background.

This paper presents a detailed multi-method assessment of glacier melt and groundwater contribution to runoff for a small catchment in the tropics. The authors find significant contributions of melting to overall runoff using tracer studies, time series analysis and hydrological modelling. They also show that melt water can be a substantial contributor to groundwater discharge. This is an excellent study that presents a thorough analysis of field data and modelling leading to interesting conclusions. The manuscript is very well written, and methods and results are clearly described. The findings are also nicely presented. Overall, I absolutely recommend this paper for publication in HESS after some mostly minor issues have been resolved (see below).

We are encouraged by the reviewer's positive comments and have carefully addressed all issues raised.

More substantive comments:

Page 5, line 11: Is there an estimate how important glacier-derived runoff is for the larger catchment? A high importance (irrigation system) is implied here, but how does the glacier runoff volume relate to larger-scale effective precipitation? Given that the absolute runoff amounts in the Gavilan Machay basin are really small (in the order of 0.1 m^3/s) I doubt that this water (despite of originating from the headwaters) has a major significance lower downstream. This is also supported by the statement of page 12, line 6. The glaciers' importance for water resources in the region might need to be better put into context.

When extended downgradient to the Boca Toma diversion point, our mixing model analysis with HBCM predicts that surficicial runoff of meltwater contributes a range of 4-15% of the discharge to the irrigation system over 2012-2017, with the rest supplied by groundwater. While this melt contribution indeed seems to comprise a minor proportion, earlier investigation by La Frenierre (2014) on downstream water usage showed that farming communities cannot afford to lose any of the water; already, the irrigation system consistently fails to deliver its current allocations. Furthermore, if groundwater at Gavilan Machay also contains meltwater, as our simulations suggest, the actual total amount of meltwater contribution could be even higher than the 4-15% estimated for surficial runoff of meltwater. A lack of model input data outside of the Gavilan Machay sub-catchment prevented further extension of the model to Boca Toma. We added this discussion to **Page 24, line 28**.

Page 9, line 23: The authors use a model that computes snow melt based on the energy balance. It is surprising to me that they nevertheless decided to implement an empirical, strongly simplified model for ice melt. This seems to be an unnecessary and also unphysical combination of approaches. Later, it is stated that a temperature index model is the only feasible approach given the limited data availability. However, if data are available to force an energy balance model for snow, it should also be applicable to glacier ice (just having a different albedo and surface roughness). More argumentation is required here, and possibly more insight into the energy balance scheme of Flux- PIHM.

We do not use energy balance calculations for glacier melt for two reasons. First, energy balance calculations of glacier melt would have to be coupled with the other energy balance calculations

already in the Flux-PIHM model (for snow-melt, ET, sensible heat flux, and ground heat flux) because of both its role in the partitioning of incoming net radiation and its effect on surface temperature. However, adding this to Flux-PIHM requires intensive source-code modifications that are beyond the scope of this study. Second, an alternative approach of an approximate, uncoupled energy balance calculation of glacier-melt would be complicated by the lack of radiation input measurements in the study watershed. We currently use GLDAS data with Flux-PIHM for its energy balance calculations, but there is substantial uncertainty in applying the coarse-scale GLDAS radiation values over the steep mountainous watershed. Because of these difficulties, we chose to invoke the simpler temperature-index model and focused on constraining glacier-melt amounts based on discharge observations at the watershed outlet. We added this explanation on **page 10, line 10**.

We do note that using coarse-scale GLDAS does introduce uncertainty into the current Flux-PIHM energy balance calculations, including for snowmelt. However, even without partitioning some of the incoming radiation for glacier melt in the model, our simulated snowmelt is a relatively small contribution of the total meltwater (15%), suggesting that precipitation limitations may make snowmelt calculations less sensitive to uncertainties in radiation inputs. This is now explained on **page 16, line 5**.

Page 9, Eq. 1: Given that relatively large parts (those experiencing the highest melt rates) of the glaciers are covered by supraglacial debris, I wonder how the model distinguishes between ice melting over these regions in comparison to clean ice.

We had reported measurements of a slower ablation rate (0.54 to 0.87 m/yr) for the insulated debris-covered ice compared to a faster rate (3.4 m/yr) for the clean ice (**page 16, line 1**), which indeed support debris-dependent melt conditions. However, these were only a handful of ablation measurements over different time periods, which were not sufficient to constrain separate melt factors for debris-covered and clean ice. We state this more explicitly now on **page 15, line 33**.

Figure 4: In my print-out (but not in the online pdf version!) there are ugly black squares around panels c and d, mostly covering the axis text. Please carefully check the figure data. Obviously, these issues only arise for particular printer drivers but make the figure almost unreadable. The same observation has also been made for Figure 8 (black squares left of the glacier snout in all panels).

We have edited the figure (now Figure 5) and hope this resolves the issue.

Page 20, line 12: Tackling the problem using different complementary approaches is highly beneficial. However, after reading the results section I somewhat missed a synthesis (figure) of the findings from the three different methodologies. For example, Fig. 3 and Fig 5 c/d could be combined to permit a direct comparison of findings based on tracers and based on the hydrological model which might also be helpful in discussing drawbacks and potentials of the individual methods.

Thank you for the suggestion. We updated Figure 6d (formerly Figure 5d) (showing model results) by shading the interval of % Melt Contribution estimated with the mixing model (from Fig. 3a) in order to facilitate comparisons between methods. We point to this shading in the text (**page 20, line 7**). The reviewer's other suggestion of adding the discharge estimates from the mixing model (from Figure 3b) to Figure 6c would likely make the plot too busy, since it already has 5 different lines. The discharge information is summarized in Figure 6d, so we think that adding the mixing model results to Figure 6d should suffice to address the reviewer's concern.

Additional detailed comments:

Page 2, line 11: normally, references are ordered with the year of appearance but not here.

Thank you. We corrected this.

Page 3, line 5: please shortly mention the physical reason (energy balance) why higher humidity leads to more ablation this might not be immediately clear to the reader.

We added the following explanation to **page 3, line 6**: "Harpold and Brooks (2018) showed that increasing humidity enhances ablation rate by increasing net longwave radiation and condensation."

Page 5, line 19: Are there observations of recent glacier retreat in this region? Just to round up the story.

We revised the following sentences on **page 5, line 1** by adding the underlined explanation: "Records since 1980 indicate that, consistent with the rest of the tropical Andes, temperatures have warmed $0.11°C$/decade around Volcń Chimborazo (Vuille et al., 2008; La Frenierre and Mark, 2017). This likely caused a 21% reduction in ice surface area and 180m increase in the mean minimum elevation of clean ice between 1986 and 2013 (La Frenierre and Mark, 2017)".

Page 5, line 27: precipitation gradients were determined with stations at 3900 and 4500 m a.s.l., respectively. Will this elevation difference be enough to capture / estimate precipitation over the higher reaches of Chimborazo, i.e. between 5000 to 6200 m a.s.l.?

Previous research in a glacierized mountainous watershed by Wang et al. (2016) found that the elevation-precipitation relationship is piecewise linear, with precipitation increasing with altitude below the elevation of maximum precipitation (EMP) and decreasing with altitude above the EMP. Such results support our application of a negative linear lapse rate calculated from our two stations - both located in the lower part of the watershed - to the higher elevation portions of the watershed. However, we should have and now do explicitly acknowledge that this assumes the EMP to be located below our watershed, which could lead to errors in the precipitation if the EMP is actually within the watershed above the lowest weather station. We point to the need for denser monitoring to better constrain the EMP and precipitation lapse rate, as well as recognize potential errors in the precipitation measurements due to wind and freezing temperatures. The assumptions and uncertainties about the precipitation spatial extrapolation approach are now discussed on **page 5, line 29**.

Page 5, line 28: It is a drawback for melt model validation that the ablation stakes are only installed over a very limited elevation range (i.e. not permitting to capture elevation gradients in glacier melt), and as it seems only over the debris-covered parts of the glaciers. This should be stated.

The ablation stakes were installed in clean ice. This had been explained previously in the Results section, but we have now also added it to the Methods section on **page 6, line 12**, where it should have been first mentioned. We also now better organized the presentation of the glacier melt measurement methods so that we explain in the next sentence (**page 6, line 16**) that we made imagery-based estimates of glacier mass loss of debris-covered ice. Later in Section 4.3.1 Calibration Results, we explain that our calibrated average glacier melt rate (below the equilibrium line altitude) is lower than the ablation stake measurements in faster-melting clean ice and higher than the mass balance measurements for the slower-melting debris-covered ice (**page 15, line 33**). We believe our reorganized discussion should now make this all clear.

Figure 7: I like the analysis of the coherences and it allows interesting conclusions to be drawn. However, it would be helpful if the term "coherence" would be better introduced, making it clearer how it was computed and what it potentially shows.

We present results for magnitude squared coherence, which can be thought of as the square of the correlation (between 0 and 1) between two variables at a certain frequency. Thus, coherencies between precipitation and discharge and between temperature and discharge indicate how strongly each of the climatic signals relate to discharge at a certain time scale. Looking at different time scales helps to distinguish whether these relationships may occur through fast surficial processes or slower subsurface processes, and whether discharge is more sensitive to certain climate forcings at particular time scales, represented by time frequencies. Mean squared coherence at time-frequency f is defined as:

$$C_{xy} = \frac{|S_{xy}(f)|^2}{S_{xx}(f)S_{yy}(f)} \tag{1}$$

where, $S_{xx}(f)$ and $S_{yy}(f)$ are auto-spectral densities of variables x and y, respectively, and $S_{xy}(f)$ is the cross spectral density of x and y. We added this explanation of coherence to the Methods section on **page 6, line 26**.

Page 19, line 12: Highly interesting finding. In how far could these 18% meltwater contribution to groundwater runoff be generalized to other catchments (different sizes, geology etc.)? Have there been other studies coming up with similar estimates or is this the first time this has been quantified? May be something for the conclusion section.

Past studies have examined the overall role of groundwater in glacierized watersheds and have found it to contribute up to 80% of total stream discharge (Clow et al., 2003; Liu et al., 2004; Huth et al., 2004; Hood et al., 2006; Baraer et al., 2009; Andermann et al., 2012; Baraer et al., 2015; Pohl et al., 2015; Somers et al., 2016; Harrington et al., 2018). A smaller number of studies have also identified a component of meltwater in the groundwater (Favier et al., 2008; Lowry et al., 2010; Minaya, 2016; Baraer et al., 2015; Harrington et al., 2018), but to our knowledge, our work is the first to quantify this component. Generalizing our results to other glacierized watersheds depends on a number of geologic and climatic factors. The importance of meltwater contributions to stream-flow through groundwater depends first on the presence of groundwater pathways. These typically are most prominent with the presence of fractures in young volcanic bedrock (Tague et al., 2008; Frisbee et al., 2011; 2014; Markovich et al., 2016) - like Chimborazo - and sometimes even crystalline bedrock (Tague et al., 2009; Andermann et al., 2012; Pohl et al., 2015). However, morainic deposits (Favier et al., 2008, Minaya, 2016, Somers et al., 2016) and alpine meadow soils (Loheide et al., 2009; Lowry et al., 2010; Gordon et al., 2015) have also proved to be effective groundwater units below glaciers and snowpacks. Even in settings that may have limited groundwater networks extending throughout the watershed, talus slopes and rock glaciers can serve as localized areas of meltwater recharge (Clow et al., 2003; Baraer et al. 2015; Harrington et al., 2018). In the groundwater, the proportion of precipitation versus meltwater depends on watershed size and climate. Well-established discharge-watershed area relationships for non-glacierized watersheds lead to predictions of increased precipitation contribution in larger watersheds (with similar glacierized areas). More arid settings may be expected to have a higher proportion of glacier-melt due to overall less precipitation inputs to the watershed, although our results indicate a possible interaction between glacial melt contributions and precipitation, where rainfall boosts melt contributions through both the transfer of heat to glaciers and through antecedent moisture conditions that facilitate meltwater recharge. We thank the reviewer for this comment, which prompted us to better highlight our new contribution and its potential implications elsewhere. We have added a paragraph about this in the Conclusions on **page 24, line 1**.

Page 22, line 22: I do not agree that runoff after glacier disappearance decreases by the current amount of melt contribution. As much as I understand, melt computed by the model includes both ice and snow melt. Whereas glacier ice melt is zero after the glacier has disappeared, snow melt is likely to remain a significant component of runoff or would be replaced by liquid precipitation in the case that the zero degree line remains above the top of Chimborazo all the time. Therefore, I would expect a significantly smaller runoff reduction for the catchment in the far future than implied here.

The reviewer's comment prompts us to make one clarification and also qualify our statement about the runoff change after the glaciers disappear. First, we clarify that the model scenario we called "No Melt" should have been called "No glacier melt", and the scenario we called "With melt" should have been called "With glacier melt" - we did correct this naming scheme in the manuscript. Both model scenarios include the same snowmelt amount, because they use the same meteorological inputs to Flux-PIHM. Flux-PIHM simulates snowmelt based on precipitation and temperature inputs, while glacier melt is simulated externally (using the temperature-index model) and then added as another water source to Flux-PIHM. Thus, our calculation of change between the two scenarios isolates the effect of having glacier melt versus no glacier melt. This is now all clarified on **page 18, line 6**. Also, we have specified "glacier melt" rather than just generic "meltwater" in all the discussion about the simulation results.

Although by design our simulation scenarios aim to separate out glacier-melt and snowmelt contributions, we do lack constraints on their individual amounts, which means that our calibrated glacier-melt contribution could incorporate precipitation-sourced meltwater not fully accounted for in Flux-PIHM's snowmelt scheme - we now acknowledge this on **page 16, line 11** and **page 18, line 12**. Further, mixing model estimates of meltwater contribution uses meltwater from the glacier tongue, which may indeed include snowmelt and melt of freshly accumulated ice - this was already mentioned previously in the modeling results section, but we now introduce it more clearly in the Field Sampling section on p. 7, line 15. Thus, we now qualify our statement in the conclusion to say that the decrease in future discharge post-glaciers (under the same precipitation conditions) may be up to 50%, and that reduction could be less depending on snowmelt (**page 25, line 5**).

Response to Reviewer 2

We would like to thank the reviewer for their time to review our paper. In this response, we have addressed the reviewer's comments by providing clarifications and indicating how we edited the manuscript. The reviewer's comments are copied with a gray background, and our responses are provided with a white background.

This paper is an excellent, in-depth exploration of multiple methods to constrain the role of meltwater in downstream hydrology, granted at a very small scale. The innovative contribution is the use of different time scales to demonstrate the interplay between melt regimes, precipitation patterns, and groundwater dynamics. There is tremendous opportunity to expand the relevance of this work in the future by applying a similar suite of methods to data from further downstream, or nested catchments.

We are encouraged by the reviewer's positive comments and have carefully addressed all issues raised.

A few overarching issues that should be more clearly addressed in the discus- sion/conclusions:

1. The 7.5 km² basin study area has offered valuable insights because of the data collection and monitoring that can be done at this scale, but it is important to acknowledge how your insights and results may translate downstream, given that your interpretations of the hydrology and implications of glacier recessions on discharge are being presented for an area in immediate proximity to the glacier terminus.

We added a discussion of the potential downstream implications of our work through two new points in the manuscript.

First, on **page 24, line 28**, we now explain that we did extend our mixing model analysis downstream of Gavilan Machay to the Boca Toma diversion point for an irrigation system. We found that the surficial glacial meltwater contribution was about 4-15% of the discharge at Boca Toma. Although this amount of meltwater appears to comprise a minor proportion of discharge, an earlier investigation by La Frenierre (2014) on downstream water usage showed that farming communities cannot afford to lose any of the water. Already, the irrigation system consistently fails to deliver its current full allocations. Furthermore, if groundwater at Gavilan Machay contains glacial meltwater, as our simulations suggest, the actual total amount of meltwater contribution could be even higher than the 4-15% estimated for surficial meltwater. A lack of model input data outside of the Gavilan Machay sub-catchment prevented further extension of the model to Boca Toma.

Second, on **page 24, line 34**, we now discuss the potential outcome of extending measurements and the model implementation downstream. Looking within our small study watershed, estimates of groundwater contribution over the stream network reveal a nonlinear relationship with subcatchment area that contains sharp increases where geologic features likely create localized discharge points (we have added the figure to the Supplementary Information). This indicates that extrapolations downstream will likely depend on geological conditions that control groundwater, in addition to watershed size and climate inputs.

2. The differentiation, or lack thereof, between snow and glacier melt should be more explicitly discussed. How big a role does snow (melt) play in the catchment, and what data to you have that informs this? To explore this, and relevant to many of your interpretations, a cursory estimate of the precipitation partition in the catchment could be interesting - what percent of precip falls as snow vs. rain based on your temperature and precip data? Given that information and your

discharge measurements, do you have a sense of relative contribution of snowmelt vs. glacier ice melt, or even how much of the discharge from the glacier terminus could also be liquid precip routed through that pour point?

We have edited the manuscript to clarify the distinction between snowmelt and glacier melt in both the mixing model analysis and watershed model simulations.

For the mixing model, the meltwater end-member was represented using the hydrochemistry of a water sample collected just below the glacier tongue - this is now clarified on **page 7, line 15**. Therefore, our estimates of meltwater contribution using the mixing model approach would include both glacier and snowmelt.

In our watershed model simulations, we aimed to distinguish glacier from snowmelt, but we realized from the reviewer's comment that we did not explain this clearly in the text. When we referred to the "With melt" and "No melt" model scenarios, we meant "With glacier melt" and "No glacier melt", respectively, because the two scenarios actually have the same amount of snowmelt; the only difference is that the former has an added glacier melt amount of water - determined with the temperature index model calibrated to discharge measurements. Apart from this glacier melt amount, both scenarios include the same meteorological inputs and thus same snowmelt amount. Through this approach, the melt contribution that we determined by differencing the two scenarios should only represent glacier melt. We have now clarified this on **page 18, line 6**.

The reviewer does make the good suggestion that we should discuss the relative snowmelt and glacier melt amounts in the model. The model Flux-PIHM simulates the partitioning of precipitation inputs between rain and snow based on air temperature. Over the 2016 period, the model predicted that about 12% of precipitation falls as snow in the watershed– this is now stated on **page 16, line 6**. The calibrated glacier melt is 567% of simulated snowmelt amount (i.e., snowmelt is 15% of the total meltwater) (now explained on **page 16, line 5**). On average, snow melt contributes 8% of stream discharge, while glacial melt contributes 52% (now stated on **page 18, line 8**).

We acknowledge that although we aim to distinguish between glacier melt and snowmelt in the model, there is uncertainty in the partitioning due to a lack of separate data constraints. Our snowmelt simulation is highly sensitive to any errors in the lapse-rate based spatial extrapolation of precipitation and temperature in the watershed, and so it is possible that our calibrated glacier melt includes some amount of snowmelt that is not captured in the Flux-PIHM simulation - this is now acknowledged on **page 16, line 11** and **page 18, line 12**.

Specific comments:

P3 L23-24: which 4 major river systems?

The four major river systems are: the Río Mocha (NE flank), Río Colorado (NW flank), Río Guano (SE flank), and Río Chimborazo (SW flank). The names of the watersheds were added to **page 3, line 23**.

P5 L5: Do you know if historically any other glaciers generated perennial surface discharge?

There are no historical streamflow data for any of Chimborazo's glacierized watersheds that are close enough to the mountain to be able to discern a glacier melt signature. Discussions with local water users by did La Frenierre (2014) not yield clear information about historic glacier meltwater flows, aside from the general observation stream and spring discharges are lower now than they have been in the past. We note the lack of historical glacier melt data on **page 5, line 5**.

P6 L10-12: Lack of any rainy/wet season samples is a limitation.

As we mentioned, mixing model analyses of melt contributions typically have been applied in the dry season in the better-studied outer tropics (**page 3, line 7**). We followed suit, because melt contribution is often of greatest interest for water resource management during times of low precipitation - this is now explained on **page 7, line 7**. We also now explain explicitly that the model simulations fill this gap to examine wet season in addition to dry season conditions (**page 7, line 8**).

Section 3.2.2: Having run same analytes in different labs in different years potentially introduces error or uncertainty. How confident are you in comparing different lab re- sults? E.g. were detection limits the same, were any lab comparisons done?

We had this same concern and had thus checked for consistency by comparing the concentrations of the different cations and anions across the different sampling periods. We found that the bulk concentrations (e.g., sum of cations in Figure 2(a) and (c)) at a certain location were similar, and that the spatial trends for each analyte were consistent across sampling periods - e.g., the concentrations generally increased moving downgradient in each sampling period. There were some systematic biases for certain analytes from a particular sampling period - e.g., February 2017 had Cl^- concentrations at all locations that were higher by a relatively consistent difference compared to other sampling periods. However, this type of systematic bias between sampling periods is unimportant, because each implementation of the mixing model is carried out only with data within a certain sampling period, ensuring that we are not combining potentially incompatible data. We now explain this in the revised manuscript (**page 8, line 4**) and include individual analyte plots over location for each sampling period in the Supplementary Information (**Figure S3**).

Figure 2: 2(a) and 2(c) read like results.

We agree, and in fact, previous Figures 2(a) and (c) with concentration results are not discussed until the beginning of Section 3 Results and Discussion. We originally thought to combine these concentration results with mixing model configuration in previous Figure 2(b) in Methods so that the reader can easily align the two. However, the reviewer's comment makes us realize that readers might prefer to see the concentration results in a separate figure in the Results section. We accordingly moved previous Figures 2(a) and (c) to a separate figure (currently **Figure 3**).

P8 L20: grammar 'is be unique'

Thank you. We corrected this.

P10 L10: how were T, P, and RH interpolated?

We used temperature and precipitation lapse rates, as described earlier in the Methods section. Relative humidity measured at the Boca Toma station was applied over the entire watershed, because we did not have measurements elsewhere. We had inadvertently omitted the explanation about relative humidity previously and have now added it to the Methods section (**page 6, line 7**). The revised text points out that discharge simulations should be less sensitive to this approximate treatment of relative humidity compared to precipitation and temperature, which directly control water inputs to the watershed. This reviewer's comment on the Results section makes us realize that we should add a reference back to the Methods section on **page 10, line 31**.

P11 L4-7: unclear here how you ultimately selected tracers for the mixing model. E.g. were thresholds applied to bivariate plots?

We clarified on **page 11, line 22** that we chose as tracers those analytes that visually showed the mixed sample falling close to the line between its two source samples based on the bivariate plots in Figures S3-S6. For example, for a tributary, the outflow sample should fall on a line between its two inflow sources. This comparison is done for all reaches and tributaries within a sampling period.

P11 L13-17: Any hypothesis on why groundwater discharge was so low in Feb 2017? Are there temps or precip events that inform this anomaly?

We intended to explain this in the text, but we now realize there was a typo. We meant to write: "However, the absolute contribution, determined by applying estimates of melt fractions to average observed weekly discharge measurements around the sampling time, was lowest in February 2017, because of significantly less total [NOT groundwater] discharge compared to the other sampling periods (Figure 4(b))." The lower total discharge was likely due to lower precipitation and temperature during the weeks around the sampling period compared to during the other sampling periods (Figure S1). We edited the manuscript to correct the typo and pointed the reader to Figure S1 (**page 12, line 2**).

Figure 4 caption, line 4: "corresponding to the"

Thank you. We corrected this.

P14 L13-15: how do these melt factors compare to the literature?

They fall within the range of melt factors calculated for other glaciers in the tropics (3.5-9.9 mm we $°C^{-1}d^{-1}$) reported in Fernandez and Mark (2016). We added this on **page 15, line 23**.

P14 L24: reference for historic geodetic mass balance estimates?

We added the explanation that glacier volume change of debris-covered ice was estimated by differencing a GPS-validated photogrammetric digital elevation model in 1997 (Jordan et al., 2008) and terrestrial laser scanner (Riegl LMS-Z620) surveys in2012 and 2013 (La Frenierre, 2016) (**page 6, line 18**). In the same section, we also noted that due to imitations in the spatiotemporal coverage of the glacier mass balance measurements, this estimate was not directly used in our model simulations but instead only served as a comparison point for our calibrated melt estimate (**page 16, line 2**).

P14 L30: missing close parentheses - "full details)."

Thank you. We corrected this.

Figure 5(d): y-axis label typo "Contribution"

Thank you. We corrected this

Figure 5 caption: clarification on "(a) average air temp below ELA (5050 m.a.s.l.) and over glaciers and simulated melt inputs" does this mean T is averaged over ablation zone plus snow covered area?

We clarified the caption for **Figure 6a** (previously Figure 5a): the figure shows T averaged over the ablation zone. We do not separately track snow-covered area, as this is highly transient in the inner tropics.

Figure 5 caption, L4: 'distribution' should be 'contribution'

Thank you. We corrected this.

P20 L10-11: what you suggest here is a buffer against lower extreme low flows during drought times, which somewhat contradicts your repeated assertion (e.g. P20 L14) that melt does not necessarily provide the buffer often credited to it. Reconciling these, perhaps with a clear acknowledgement in the conclusions that the buffer does exist for extreme low flow scenarios, but the modulating effect in other flow scenarios may not be as strong of a control on streamflow as other studies suggest.

Thank you, this is a very good point. You captured exactly what we meant. We revised the text to clarify our conclusion that the classic paradigm that melt buffers does not always apply, though it still can buffer against extreme low discharge periods (**page 22, line 9**).

P20 L26-27: these longer periods controlled by melt inputs are via infiltration and groundwater recharge, right?

No, in fact we are talking about 30-80 day discharge patterns being driven by 30-80 day melt production patterns. We realize this is not an obvious connection, since we also talked about melt contributions to discharge being a fast (hourly time scale) process. But, this finding emerged from the coherence analysis (Figure 8). We clarified this in a few ways. First, we clarified the text where this connection was originally discussed with reference to coherence results, on **page 20, line 15**. Here, and through-out, we edited the wording to clarify connections between melt "production" (instead of the former wording of "melt input") versus melt contribution to discharge. In this particular line, we explicitly point to the coherence plot to show that there is a strong correlation at 30-80 day periods between glacier melt production and glacier melt contribution to discharge. In the following lines in that section, we more explicitly acknowledge that even though this is a dynamic at longer multi-month timescales, it is nonetheless occurring through surface runoff of meltwater. Second, we reworded the sentence in question in the Conclusion section so that it now reads: "Coherence analysis of the model results showed that not only were diurnal discharge patterns responding to radiation-driven melt inputs, but relative melt contribution and discharge variations over 30-80 day periods were controlled by extended glacier melt production periods that also contribute to discharge through surface runoff (Figure 9(c))." In particular, we reminded the reader that this came from the coherence analysis. We also emphasized that we are talking about longer periods of melt ("extended") and that we are talking about melt production and not vaguely melt "inputs."

Figure 8 caption, lines 1-2: reference here to glacial meltwater is misleading, since what you've characterized is glacier outflow that is a combo of ice and snow melt, right?

No, what we represented here is only the result of glacier meltwater, since the same snowmelt amount was present in both the "With melt" and "No melt" simulation scenarios. As stated in an above response, we realized that we should have called the "No melt" scenario "No glacier melt", because it only removed glacier melt. See our response above to your overarching issue #2 for how we clarified this.

P22 L9: "Recharge by meltwater"

Thank you. We corrected this.

P22 L22-23: Unclear what justifies the assertion that discharge could be reduced by half. Equilibrium discharge with glacier melt contributions and equilibrium discharge post-glaciers should be the same if precip is the same, barring other changes (e.g. increased ET). The peak water period in the middle is a different story, but this claim seems unsupported.

As mentioned in Section 2 Study Area, the glaciers on Chimborazo are already retreating fast and

5

thus are not in equilibrium. This leads us to consider the glacial meltwater as originating largely from stored ice from earlier time periods. In fact, our calibrated glacier melt input is addition to precipitation inputs, so we consider it to represent melt of pre-existing ice at the start of the model run - this is now explained on **page 18, line 10**. However, the reviewer makes a good point that even during peak water period (when ablation $\succ$ accumulation), some of the meltwater could still originate from newly accumulated ice, such that post-glaciers, this amount of water would still fall as precipitation and contribute to discharge. We edited our manuscript to clarify that without glaciers, but assuming the same precipitation, the potential future reduction of discharge by half is an upper limit, and that the reduction could be less if some of current-day precipitation goes to glacier accumulation, or if the estimated current meltwater contribution includes snowmelt (**page 25, line 5**).

P22 L24-25 Related to the previous comment and as mentioned at the beginning, the other huge caveat is that you are looking at a point 2km from a glacier terminus, so results absolutely cannot be implied to inform understanding of vulnerability of water resources. Extrapolating further downstream is a logical next step and I think expanding your methods downstream would be an incredibly valuable contribution to this understanding!!!

We agree that it would be extremely valuable to extend our work downstream, now that we have established this multi-method approach. As described in our response to the reviewers overarching issue #1, we did apply the mixing model to the irrigation diversion point Boca Toma downstream from the Gavilan Machay discharge point. The findings and implications are provided in that first response. We were not able to extend the model over the entire Boca Toma watershed (26 km^2) due to the unavailability of weather input data for that other portion of the watershed outside of the Gavilan Machay watershed. Also, the other part does not have glacier melt, and so working on Gavilan Machay allows us to focus on the glacier contribution to the irrigation system.

Multi-scale temporal variability in meltwater contributions in a tropical glacierized watershed

Leila Saberi[1], Rachel T. McLaughlin[1], G.-H. Crystal Ng[1,2], Jeff La Frenierre[3], Andrew D. Wickert[1,2], Michel Baraer[4], Wei Zhi[5], Li Li[5], and Bryan G. Mark[6]

[1]Department of Earth Sciences, University of Minnesota - Twin Cities, Minneapolis, MN 55455, USA
[2]Saint Anthony Falls Laboratory, University of Minnesota - Twin Cities, Minneapolis, MN 55455, USA
[3]Department of Geography, Gustavus Adolphus College, St. Peter, MN 56082, USA
[4]Construction Engineering, École de Technologie Supérieure, Université du Quebec, Montreal, Canada H3C 1K3
[5]Department of Civil & Environmental Engineering, Pennsylvania State University, University Park, PA 16802-1294, USA
[6]Department of Geography, The Ohio State University, Columbus, OH 43210-1361, USA

Correspondence: Leila Saberi (saber017@umn.edu)

Abstract. Climate models predict amplified warming at high elevations in low latitudes, making tropical glacierized regions some of the most vulnerable hydrological systems in the world. Observations reveal decreasing streamflow due to retreating glaciers in the Andes, which hold 99% of all tropical glaciers. However, the timescales over which meltwater contributes to streamflow and the pathways it takes – surface and subsurface – remain uncertain, hindering our ability to predict how shrinking glaciers will impact water resources. Two major contributors to this uncertainty are the sparsity of hydrologic measurements in tropical glacierized watersheds and the complication of hydrograph separation where there is year-round glacier melt. We address these challenges using a multi-method approach that employs repeat hydrochemical mixing model analysis, hydroclimatic time series analysis, and integrated watershed modeling. Each of these approaches interrogates distinct timescale relationships among meltwater, groundwater, and stream discharge. Our results challenge the commonly held conceptual model that glaciers buffer discharge variability. Instead, in a sub-humid watershed on Volcán Chimborazo, Ecuador, ~~meltwater~~ glacier melt drives nearly all the variability in discharge (Pearson correlation coefficient of 0.89 in simulations), with glaciers contributing a broad range of 20-60% or wider of discharge, mostly (86%) through surface runoff on hourly timescales, but also through infiltration that increases annual groundwater contributions by nearly 20%. We further found that rainfall may enhance glacier melt contributions to discharge at timescales that complement ~~melt generation~~ glacier melt production, possibly explaining why minimum discharge occurred at the study site during warm but dry El Niño conditions, which typically heighten melt in the Andes. Our findings caution against extrapolations from isolated measurements: stream discharge and ~~meltwater~~ glacier melt contributions in tropical glacierized systems can change substantially at hourly to interannual timescales, due to climatic variability and surface to subsurface flow processes.

1 Introduction

Glaciers supply water resources to over 600 million people worldwide (Messerli et al., 2004). By melting during dry seasons and drought years, they supplement streamflow (Fountain and Tangborn, 1985; Lang, 1986; Escher-Vetter et al., 1994; Jansson

et al., 2003; Juen et al., 2007; Soruco et al., 2015; Chen et al., 2017) and ensure reliable water supplies (Mark and Seltzer, 2003; Mark and Mckenzie, 2007; Bury et al., 2013). This has led to the commonly held conceptual model, called the "glacier compensation effect" (Lang, 1986), in which meltwater buffers discharge variability.

Climate change can disrupt the glacier compensation effect, and tropical glacierized watersheds that already experience year-round melt (Kaser and Osmaston, 2002) may be the most vulnerable. Climate models predict amplified temperature increases at high altitudes in low latitudes (Bradley, 2006; Pepin et al., 2015). The retreat of these glaciers temporarily results in increased runoff (Braun et al., 2000; Mark, 2008; Polk et al., 2017; Carey et al., 2017), but gradually depletes the storage of these mountain "water towers". Over time, this reduction in storage capacity can render these glaciers unable to supply sufficient dry-season meltwater discharge for the communities that depend on it (Barnett et al., 2005; Bradley, 2006; Mackay, 2008; Ostheimer et al., 2005; Luce, 2018). Indeed, observations already reveal reduced and fluctuating flows in glacierized watersheds (Mark and Seltzer, 2003; Huss et al., 2008; Baraer et al., 2012; Rabatel et al., 2013; Baraer et al., 2015; Soruco et al., 2015), threatening the water security of millions of people ~~(Carey et al., 2017; Immerzeel et al., 2010; Vuille et al., 2018)~~(Immerzeel et al., 2010; C

Of all glaciers in the tropics, 99% are located in the Andes (Kaser, 1999), often in remote regions, where resource-limited populations often rely on their meltwater (Bury et al., 2011; La Frenierre and Mark, 2017). Despite over a decade of research ~~conducted~~ in Peru's heavily glacierized Cordillera Blanca (Mark and Seltzer, 2003; Mark and Mckenzie, 2007; Juen et al., 2007; Mark et al., 2005; Baraer et al., 2012, 2015), many of the processes linking variability in climate, glacier melt, and stream discharge remain uncertain. For example, groundwater is also a major contributor to discharge in many glacierized mountainous watersheds around the world ~~(Tague et al., 2008; Tague and Grant, 2009; Andermann et al., 2012; Baraer et al., 2015; Markovich et al., 20~~ This can further modulate discharge through baseflow~~(Jasechko et al., 2016; Staudinger et al., 2017). However,~~, but its capacity to do so as glaciers respond to climate change is complicated by largely unconstrained relationships between glacial meltwater and groundwater recharge ~~(Favier et al., 2008a; Baraer et al., 2015; Gordon et al., 2015)~~(Favier et al., 2008a; Baraer et al., 2015; Gordo

Understanding how different surface and subsurface pathways influence the timing of meltwater and groundwater contributions to streamflow is critical for predicting how climate change will impact the reliability of watershed discharge. A major challenge in evaluating these spatiotemporal effects in tropical glacierized watersheds is the relative data sparsity and resource limitations in these regions ~~when~~ compared to better instrumented mountainous systems in North America and Europe. ~~Because of these constraints, many~~ Many studies in tropical and other remote glacierized settings rely on focused field campaigns using methods such as synoptic water chemistry tracer sampling (Mark and Mckenzie, 2007; Baraer et al., 2009, 2015; Wilson et al., 2016), but these provide only snapshots of the hydrologic state. Even though physically based hydrologic models can provide greater spatiotemporal coverage in mountainous settings (e.g., Suecker et al., 2000; Liu et al., 2004; Tague et al., 2008; Tague and Grant, 2009; Lowry et al., 2010, 2011; Markovich et al., 2016; Pribulick et al., 2016; Omani et al., 2017; He et al., 2018), their application is relatively limited in ~~most Andean watersheds (implementations include work by Buytaert and Beven, 2011; Minaya, 2016; Omani et al., 2017; Ng et al., 2018)~~ Andean watersheds (previous implementations include work by Buytaert and Beven, 2011; Minaya, 2016; Omani et al., 2017; Ng et al., 2018) due to the lack of extensive monitoring infrastructure. With these obstacles, there remains limited understanding of how stream dis-

charge in tropical glacierized watersheds varies over time scales ranging from hours to years, and how this variability is driven by dynamic inputs of glacial meltwater and precipitation through a combination of surficial and subsurface pathways.

In this study, we probe the multiple time scales of hydrological processes in a sub-humid glacierized watershed on Volcán Chimborazo in the tropical Ecuadorian Andes. Prior to this work, there have been no comprehensive efforts on Chimborazo to quantify glacier melt as a component of watershed discharge. In contrast to the well-studied crystalline-cored Cordillera Blanca in the outer tropics, Chimborazo is a stratovolcano located in the inner tropics, and therefore experiences less-pronounced seasonality in precipitation (Kaser and Osmaston, 2002) and more persistent ablation due to higher humidity (Vuille et al., 2003; Favier, 2004; Harpold and Brooks, 2018). Higher humidity can enhance ablation rates by increasing net longwave radiation and condensation (Harpold and Brooks, 2018). Most mixing model analyses of melt contributions in the outer tropics have been limited to the dry season, leaving wet season effects less well understood. In the inner tropics, coincident glacier melt and precipitation inputs throughout the year could lead to multiple processes simultaneously driving discharge variability — likely at diverse timescales — that are difficult to disentangle. Furthermore, Andean volcanoes may feature fractured bedrock aquifers that support greater groundwater storage and baseflow than those in crystalline-cored mountainous watersheds (Tague and Grant, 2009; Markovich et al., 2016), adding another factor to be reconciled. A growing body of work at Volcán Antisana, also located in the inner tropics, has begun to shed light on its hydrogeologic (Favier, 2004; Caceres et al., 2006; Favier et al., 2008b; Cauvy-Fra ecohydrologic (Minaya, 2016) conditions, but comprehensive understanding of mountain hydrology in the inner tropics still greatly lags that in the outer tropics.

Here, we implement diverse field and computational methods to answer two questions: (1) What is the temporal variability of relative meltwater glacier melt contributions to discharge, from hourly to multi-year time scales, in a sub-humid glacierized watershed on Volcán Chimborazo? (2) What hydroclimatic factors control this variability? Our approach comprises three methods: mixing model analysis applied to repeat synoptic sampling, time series analysis of hydroclimatic data, and numerical watershed modeling. Each method interrogates a distinct temporal relationship, and synthesizing their results illuminates how the dominant surface and subsurface processes driving the hydrological response of a tropical glacierized watershed vary as a function of time scale.

2   Study Area

Volcán Chimborazo is a glacierized stratovolcano in Ecuador (Figure 1(a)) whose glaciers serve as the headwaters for four major river systems – the Rio Mocha (NE flank), Rio Colorado (NW flank), Rio Guano (SE flank), and Rio Chimborazo (SW flank) – that supply water to a population of over 200,000 (INEC, 2010). Located in the inner tropics, Chimborazo's climate is characterized by minimal intra-annual temperature variation ($\sim 2°$C) and moderately seasonal precipitation, with two wetter seasons of unequal length (February-May and October-November) (Clapperton, 1990), and two intervening drier seasons that have less but not negligible amounts of precipitation. Moisture mostly originates from the Amazon Basin to the east (Vuille and Keimig, 2004; Smith et al., 2008), which produces a steep northeast (up to 2000 mm/yr) to southwest (<500 mm/yr) precipitation gradient across the mountain (Clapperton, 1990). Driving interannual climatic variability at the regional scale,

El Niño generally brings drier and hotter conditions throughout the Andes (Vuille and Bradley, 2000; Wagnon et al., 2001; Francou, 2003; Bradley et al., 2003; Vuille and Keimig, 2004; Smith et al., 2008), which enhances glacier ablation (Wagnon et al., 2001; Favier, 2004; Veettil et al., 2014b).

Records since 1980 indicate that, consistent with the rest of the tropical Andes, temperatures have warmed 0.11°C decade^{-1} around Volcán Chimborazo (Vuille et al., 2008; La Frenierre and Mark, 2017). This likely caused the 21% reduction in ice ~~area since~~ surface area and 180 m increase in mean minimum elevation of clean ice observed between 1986 and 2013 (La Frenierre and Mark, 2017). Although regional precipitation gauges show no notable change over time, local residents report a reduction in precipitation, which could further drive glacier mass balance changes (La Frenierre and Mark, 2017). Historical records of glacier melt are not available. Under current conditions, only four of Chimborazo's seventeen glaciers, including the two largest, Reschreiter (2.55 km^2) and Hans Meyer (1.33 km^2), generate perennial surface discharge, nearly all of which flows northeast into the Río Mocha watershed. The lowest 16% of Reschreiter Glacier is debris-covered, providing insulation that stabilizes ice at lower elevations (4480 m.a.s.l) than would be expected for clean ice, given current climatic conditions. Our study focuses on the 7.5 km^2 Gavilan Machay sub-catchment on the sub-humid northeast ~~flanks~~ flank of Chimborazo (Figure 1(b)), which is 34% glacierized by Reschreiter and is of concern because it discharges into the main Río Mocha channel just upstream of the Boca Toma diversion point (3895 m.a.s.l. elevation) for an irrigation system.

In addition to glacier melt, groundwater and ecological conditions also control the hydrology of the Gavilan Machay watershed. Springs are prevalent below 4400 m.a.s.l. Geologic maps and stratigraphic interpretations (Barba et al., 2005; Samaniego et al., 2012) support field evidence for aquifers within unsorted glacial deposits and underlying fractured bedrock (McLaughlin, 2017). Extensive areas of páramo, the biologically rich grasslands endemic to the tropical Andes above ∼3500 m.a.s.l., are common across the watershed. Wet páramos commonly contain homogeneous Andosol soils of volcanic origin that can accumulate elevated organic carbon content; this typically gives rise to high porosity, infiltration capacity, hydraulic conductivity, and water retention (Buytaert et al., 2006; Buytaert and Beven, 2011). Absorbent páramo soils are considered to very efficiently regulate watershed discharge throughout Andean Ecuador (Buytaert et al., 2006; Buytaert and Beven, 2011; Minaya, 2016).

3 Methods

3.1 Hydroclimatic Data

Precipitation, temperature, and relative humidity data were collected from October 2011 to February 2017 from weather stations installed at 4515 m.a.s.l on the debris-covered portion of Reschreiter Glacier and at 3895 m.a.s.l. at Boca Toma (Figure S1). Logistical obstacles prevented instrumentation of the upper three-quarters of the watershed above Reschreiter. The Boca Toma weather station was deployed with an Onset Hobo Pendant® Event Logger starting June 16, 2015. The Reschreiter weather station was deployed with an Onset Hobo Micro Station starting October 2011, but temperature and precipitation data recovery was discontinuous. The short data records from Reschreiter were primarily used together with Boca Toma data to determine ~~lapse rates for precipitation.~~ a lapse rate for precipitation. Precipitation in mountainous watersheds typically exhibit piecewise linear relationships with elevation, with positive (negative) lapse rates below (above) the elevation of maximum
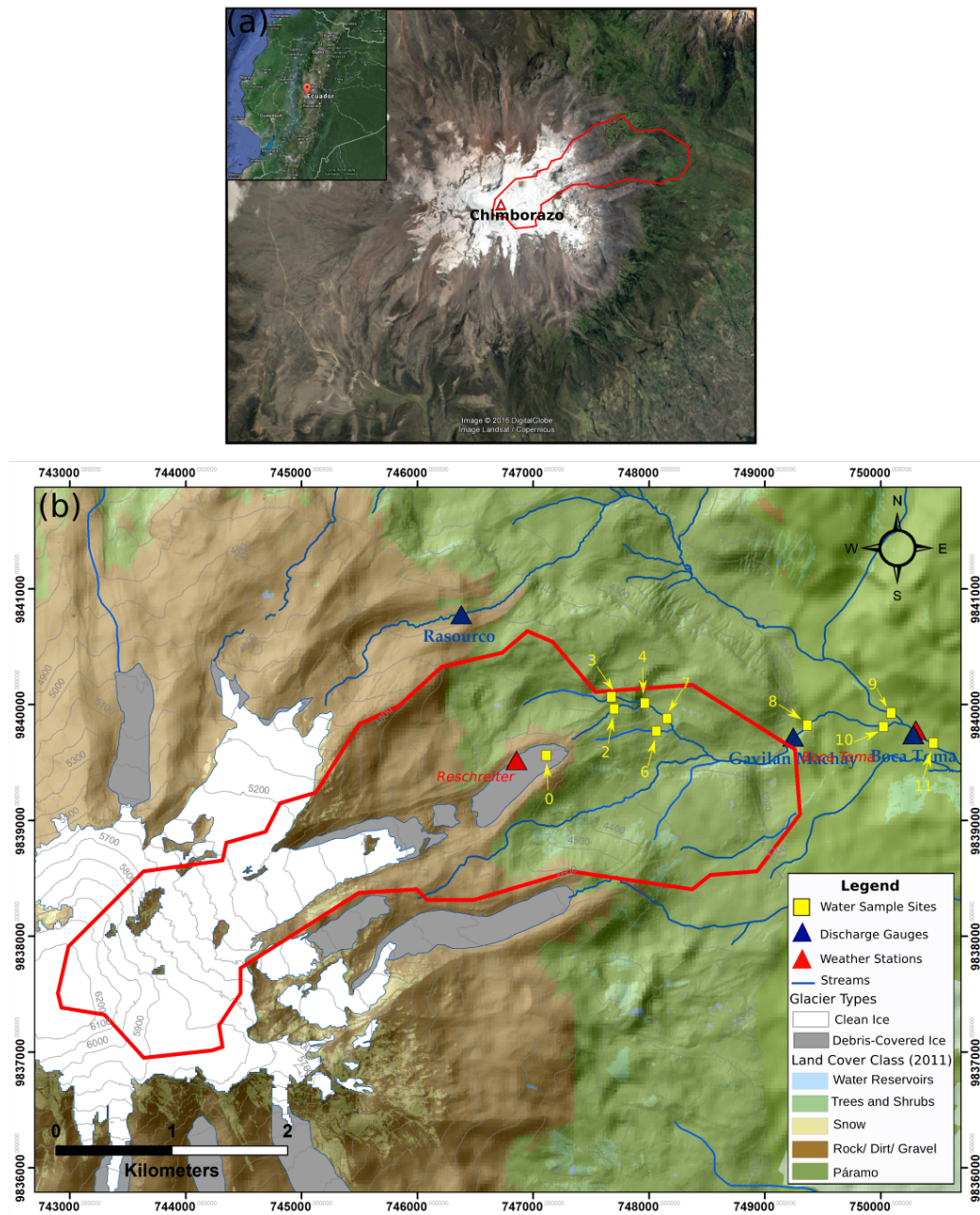
4

Figure 1. (a) Satellite image of Volcán Chimborazo, with the study watershed Gavilan Machay outlined in red, and its location in Ecuador shown in the inset map. The glacierized Gavilan Machay watershed is a relatively humid watershed compared to the western ~~flanks~~ flank of Chimborazo. **(b)** Land cover and locations of monitoring ~~station~~ stations and water ~~sample locations~~ sampling within the Gavilan Machay watershed.

precipitation (Wang et al., 2016). We calculated a negative lapse between the two weather stations, which we applied over the entire watershed with the assumption that the elevation of maximum precipitation lies below the watershed. Uncertainty in this approach arises from the actual unconstrained elevation of maximum precipitation (which requires more than two weather stations), and from unquantified precipitation measurement errors that may be caused by wind and freezing temperatures at

5 high elevations. Glacier melt was separately estimated through model calibration to stream discharge data (Section 3.3), which may compensate for errors in the precipitation inputs. Temperature lapse rates were calculated using data collected at glacier ablation stakes (described further below) over June 2016 to November 2016. Relative humidity measured at the Boca Toma station was applied over the entire watershed due to the lack of measurements elsewhere. Discharge simulations should be less sensitive to errors in relative humidity compared to precipitation and temperature, which directly control water inputs

10 to the watershed. We obtained unmeasured meteorological variables (wind speed, solar radiation, longwave radiation, and air pressure) from the Global Land Data Assimilation Systems (GLDAS) (Rodell et al., 2004). A discharge gauging station equipped with a Solinst Levelogger Junior pressure transducer was established at Gavilan Machay, 1.1 km upstream of the Río Mocha confluence. Solinst Barologger measurements at Boca Toma were applied to correct for atmospheric pressure, and standard USGS rating curve techniques (Andrews, 1981a, b) were used to convert water depth to discharge over the period of

15 record (Figure S1).

In June 2016, glacier ~~ablations~~ ablation stakes were installed at two elevations on the Reschreiter Glacier tongue (4792 and 4820 m.a.s.l.) and one on the Hans Meyer Glacier tongue (4925 m.a.s.l.), all in clean ice. Each stake included a temperature sensor, along with a look-down ultrasonic sensor for measuring changes in distance to the ice surface to estimate glacier mass loss in clean ice. The stakes were deployed using the open-source Arduino-based ALog data logger (Wickert, 2014). All sen-

20 sors were mounted at the top of 3 m long PVC tubes, which were inserted into holes drilled to about 2.5 m depth. ~~Temperature lapse rates were calculated using data collected on the glacier ablation stakes over June 2016 to November 2016. We obtained unmeasured meteorological variables (wind speed, solar radiation, longwave radiation,~~ In addition to the clean-ice mass loss determined with ablation stakes, glacier volume change of debris-covered ice was estimated by differencing a GPS-validated photogrammetric digital elevation model in 1997 (Jordan et al., 2010) and terrestrial laser scanner (Riegl LMS-Z620) surveys

25 in 2012 and ~~air pressure) from the Global Land Data Assimilation Systems (GLDAS) (Rodell et al., 2004). A discharge gauging station equipped with a Solinst Levelogger Junior pressure transducer was established at Gavilan Machay, 1.1 km upstream of the Río Mocha confluence. Solinst Barologger measurements at Boca Toma were applied to correct for atmospheric pressure, and standard USGS rating curve techniques (Andrews, 1981a, b) were used to convert water depth to discharge~~ 2013 (La Frenierre, 2016). Because of the sparse spatiotemporal coverage of these glacier melt measurements, these were used only

30 as comparisons for calibrated glacier melt and were not directly applied in our analysis.

Hydroclimatic data collected in the watershed were directly assessed using statistical analyses and implemented as inputs to the integrated hydrologic model. For the statistical analysis, we calculated cross-correlations to probe how the discharge time series may be driven by different climatic factors. Spectral analysis provided further insight on the time scales, represented by time-frequency, over which these interactions occur. Specifically, we examined the magnitude squared coherence (C_{xy}) over

~~the period of record (Figure S1)~~ time-frequency (f):

$$C_{xy}(f) = \frac{|S_{xy}(f)|^2}{S_{xx}(f)S_{yy}(f)}, \tag{1}$$

where $S_{xx}(f)$ and $S_{yy}(f)$ are auto-spectral densities of variables x and y, respectively, and $S_{xy}(f)$ is the cross spectral density of x and y. Like the square of a correlation, the magnitude squared coherence varies between 0 and 1, with 0 indicating the weakest relationship between the two variables at frequency f and 1 indicating the strongest relationship.

3.2 Hydrochemical and Isotopic Tracers

3.2.1 Field Sampling

Water samples were collected for use in the Hydrochemical Basin Characterization Model (HBCM) (~~details in Section 3.3~~ Section 3.2.3), a hydrochemical mixing model that spans the stream network and requires synoptic water sampling over a sufficiently short time period such that data reflect spatial and not temporal variability. We carried out five synoptic sampling campaigns during January 1-8, 2012; July 7-9, 2012; June 12-15, 2015; June 25-30, 2016; and February 4-7, 2017. The June and July (January and February) samples represent the longer (shorter) dry season. Dry seasons were targeted because of water resource interests during these periods; integrated hydrologic model simulations served to extend the analysis to dry seasons. In addition to limiting the number of ~~sampling days~~ days spanned during a sampling campaign, synoptic sampling should avoid hourly timescale hydrochemical fluctuations. All samples were collected between mid-morning and mid-afternoon. In February 2017, we confirmed that 1-minute resolution specific conductivity changes over a 24-hour time period at the Reschreiter glacier tongue were an order of magnitude smaller than the spatial variability across the Gavilan Machay subcatchment (details in McLaughlin, 2017). Logistical difficulties prevented similar measurements farther downstream in the watershed, where dynamic melt versus groundwater contributions likely caused greater hydrochemical variability (~~discussed further in~~ Section 4.1).

During each of the five campaigns, we collected water samples from ~~glacial meltwater,~~ meltwater, which may contain both glacier melt and snowmelt, springs, and precipitation, as well as at stream confluence mixing points (locations shown in Figure 1(b)), ~~as well as at stream confluence mixing points~~. Spring samples from concrete capture boxes or natural valley wall seeps represent groundwater, which consists of an unconstrained mix of shallow saturated soil water from páramo areas, morainic debris aquifer water, and deeper fractured bedrock aquifer water. Precipitation samples were collected using evaporation-proof totalizing rain gauges deployed for 3-6 days at Boca Toma, near the Reschreiter weather station, and near Hans Meyer glacier (at 4780 m.a.s.l.). Each field campaign covered most of the same sampling locations between the Reschreiter glacier tongue and the Gavilan Machay confluence. The 2012 and 2017 sampling periods included additional stream samples between some confluences to estimate groundwater contributions along shorter stream reaches (~~schematics in~~ Figure 2(b)). For each sampling site, 30mL of water were collected, filtered in the field using either 0.45 μm (before 2017) or 0.2 μm (2017) filters, and stored in Nalgene bottles that were capped and sealed with electrical tape, and then stored near 4°C as soon as possible.
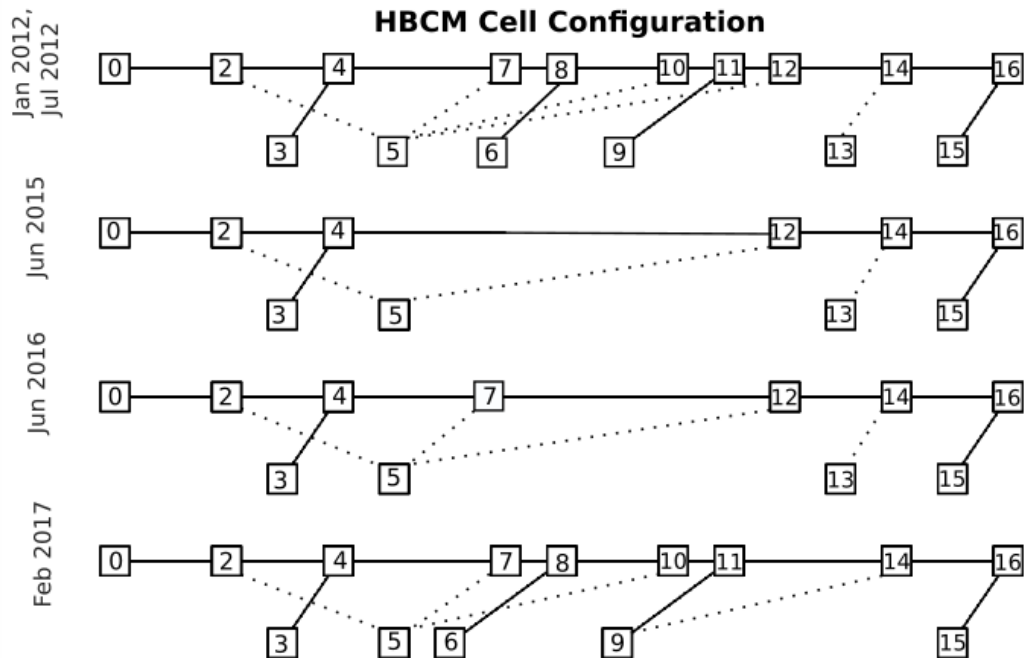
Figure 2. ~~(a) Hydrochemistry at different sampling locations along the Gavilan Machay main channel shows variability in space and over the five sampling periods; site codes are ordered from highest (0 for meltwater) to lowest (16 for Boca Toma) elevation (see Figure 1(b)). (b)~~ Different computational cell configurations for the HBCM mixing model based on the available samples (site codes in squares, see Figure 1) for each of the five periods. The upper solid ~~lines~~ line for each period ~~represent~~ represents the main channel. The lower solid lines depict tributary links for confluence cells, and the lower dotted lines show groundwater inputs to the main channel for reach cells. ~~(c) Hydrochemistry for different tributary and groundwater (spring) samples, ordered from highest to lowest elevation, show variability in space and time.~~

3.2.2 Laboratory Analysis

In 2012, major dissolved ions (Li$^+$, Na$^+$, K$^+$, Mg^{2+}, Ca^{2+}, F$^-$, Cl$^-$, NO$_3^-$, PO$_4^{3-}$ and SO$_4^{2-}$) were measured using a Dionex DX500 Ion Chromatographer at the Water Isotope and Nutrient Laboratory at The Ohio State University, and stable isotopes of water (δ18O and δ2H) were measured using Piccaro L2130-i CRDS isotope analyzers at the Water Isotope and Nutrient Laboratory and at the Byrd Polar Research Center. In 2015-2017, cations (Na$^+$, K$^+$, Mg^{2+}, Ca^{2+}) were measured using an Agilent 7700X Inductively Coupled Plasma-Mass Spectrometer (ICP-MS) at Gustavus Adolphus College, anions (F$^-$, Cl$^-$, SO$_4^{2-}$) were measured using a Dionex ICS1000 Ion Chromatographer (IC) also at Gustavus Adolphus College, and stable isotopes of water (δ^{18}O and δ^2H) were measured at the University of Minnesota using an LGR DLT-100 Liquid Water Analyzer (a laser spectroscopy system). We calculated the bicarbonate (HCO$_3^-$) concentration as the charge balance residual. Reported isotope ratios are relative to the Vienna Standard Mean Ocean Water (VSMOW) and typical precisions are ±1.0‰ for deuterium/hydrogen values and ±0.25‰ for ^{18}O/^{16}O values. Checking for consistency across instruments, we confirmed that bulk concentrations at each location and spatial trends for each analyte were similar across sampling periods (Figure S3). Certain analytes did exhibit

a discernible systematic bias for one particular sampling period compared to other periods that may be related to laboratory instrument, but this should not pose a problem for the mixing model, which is implemented only using data within the same sampling period (measured on the same instrument).

3.2.3 Mixing Model: Hydrochemical Basin Characterization Model (HBCM)

5   Naturally occurring dissolved ions and stable isotopes of water (δ^{18}O and δ^2H) have long been used to track the relative contributions of different surface source waters to total watershed discharge (Hooper and Shoemaker, 1986; Mark and Seltzer, 2003; Ryu et al., 2007; Mark and Mckenzie, 2007; Baraer et al., 2009), as well as to identify groundwater flow paths (Clow et al., 2003; Kendall et al., 2003; Baraer et al., 2009; Crossman et al., 2011; Baraer et al., 2015). Here, the proportion of glacier and snow melt versus groundwater in discharge at the Gavilan Machay watershed is quantified using the Hydrochemical

10   Basin Characterization Model (HBCM), a multi-component hydrochemical mixing model developed for use in data-sparse, glacierized tropical watersheds (Baraer et al., 2009). Given source (or "end-member") and outflow chemistries at different mixing points throughout the watershed, HBCM solves an over-constrained set of mass balance equations for multiple tracers (ion concentrations or stable water isotope values) to determine the relative flow contributions of each source. Details are provided in the Supplementary Information (HBCM Section).

15   As with all hydrochemical mixing models, HBCM's calculation of relative source contributions depends on three fundamental assumptions: (1) end-member chemistry is be unique and spatially homogeneous within the analysis area, (2) tracers are chemically conservative within the analysis, and (3) end-member mixing is instantaneous and complete (Christophersen et al., 1990; Soulsby et al., 2003). A unique feature of HBCM is that it represents spatial information within a watershed through a series of cells that are interconnected by having outflow from one become inflow to a subsequent downstream cell. There are

20   two types of cells, both of which have streamflow at the upgradient end of the cell as a source and streamflow at the downgradient end of the cell as the mixed water output. "Reach cells" have groundwater as their other source, and "confluence cells" have tributary water as their other source (see cartoon in Figure S2). Note that this makes end-members for a particular HBCM cell different than for the full watershed, which has only meltwater and groundwater as sources contributing to discharge at the outlet. Figure 2b shows the conceptual schematics of the Gavilan Machay cell configuration for the five sampling periods.

25   Although HBCM only requires the three assumptions to be met on a cell-scale, we carried out a preliminary watershed-level analysis considering groundwater and meltwater as sources to all mixed stream samples, in order to identify potential conservative tracers that are reasonable candidates for all cells. Appropriate tracers should show end-members appearing on opposite ends of a line formed by mixed samples in bivariate plots, and samples for different end-members should group separately from each other in hierarchical cluster analysis diagrams (Christophersen et al., 1990; Hooper, 2003; James and

30   Roulet, 2006). Stable isotopes were excluded as tracers for reach cells, because the groundwater likely has a range of isotopic values due to different recharge elevations.

To bracket some of the uncertainty in the method, HBCM generates estimates of fractional contributions from each source using different combinations of potential tracers. The final result consists of a range of estimates that produce similar (within about three times the minimum) cumulative residual errors between the measured tracer concentrations in the mixed outflow

9

water and that predicted by the over-constrained mixing model. This quantifies uncertainty due to the model's inability to distinguish among equally good optimization results ~~, but it should be noted that this~~ but represents only a lower limit of error, because it does not account for the mismatch between the observed and predicted mixed concentration outflows. There are no straightforward methods to convert the sum of residual concentration flux errors to estimated source contribution errors.

3.3 Integrated Hydrologic Modeling

Spatially distributed watershed models can integrate surface hydrology and groundwater flow through time to evaluate their joint impacts on water resources. Over the one-year period of June 2015-June 2016 when continuous air temperature and precipitation measurements are available in the watershed, we ~~implement~~ implemented Flux-PIHM (Shi et al., 2013), an intermediate complexity watershed model that balances mechanistic parameterizations with computational efficiency. Full details about Flux-PIHM can be found in Qu and Duffy (2007) and Shi et al. (2013); here, we summarize the major features. Flux-PIHM couples physically based equations for canopy interception, infiltration, surface and subsurface water flow, and snow melt with the energy balance scheme of the NOAH land-surface model (Ek et al., 2003) for more accurate simulation of evapotranspiration. Flux-PIHM employs a semi-discrete finite volume approach on an unstructured grid that performs efficiently on steep topographies. Channel and overland flow are represented by diffusion wave approximations to St. Venant equations; shallow groundwater flow follows a ~~2-D~~ 2D Dupuit approximation; and unsaturated zone flow is based on a 1D form of Richards equation. The model simulates water storage in one vertically integrated unsaturated zone layer and one vertically integrated saturated zone layer, providing a "2.5D" distributed model.

Flux-PIHM ~~calculates~~ determines snowmelt based on energy balance. ~~We added another~~ Use of coarse-scale GLDAS radiation inputs introduces errors, but as will be discussed in Section 4.3.1, precipitation limitations may make snowmelt calculations less sensitive to radiation input uncertainties compared to glacier melt calculations. Due to the unavailability of high resolution radiation input measurements as well as intensive source-code modifications required to couple energy balance calculations for ice melt into the Flux-PIHM, we added a separate module to simulate glacier melt using a ~~temperature-index (TI) scheme (NRCS, 2009)~~ temperature index scheme (NRCS, 2009). Although the accuracy of a temperature index glacier melt model for tropical glaciers can be uncertain due to uncaptured effects of solar radiation, cloud cover, humidity, topography, and aspect (Hock, 1999, 2005; Pellicciotti et al., 2005; Sicart et al., 2008; Huss et al., 2009; Gabbi et al., 2014; Fernández and Mark, 2016), it remains the most feasible approach in poorly instrumented watersheds given its simplicity and limited field data requirement compared to an energy balance approach (Hock, 2005; Fernández and Mark, 2016; Reveillet et al., 2017). The temperature index glacier melt model includes:

$$F_I = M_I(T_a - T_{M,I}) \qquad T_a > T_{M,I} \tag{2a}$$

$$F_I = 0 \qquad T_a < T_{M,I} \tag{2b}$$

10

where F_I is the ice melt rate (m/hr), ~~Ta~~ T_a is air temperature in the grid cell containing ice (°C), M_I is the melt factor parameter (m/hr/°C) to be calibrated, and $T_{M,I}$ (°C) is set to 0°C as the air temperature threshold for ice to melt. Over the simulated time period, we assume that there is an unexhausted supply of ice that can melt in the glaciated grid cells below the equilibrium line altitude (ELA) at 5050 m.a.s.l. (Frenierre and Mark, 2014), which is a reasonable approximation over the one-year simulation

5 period. The ~~accuracy of a temperature index glacier melt model for tropical glaciers can be uncertain due to uncaptured effects of solar radiation, cloud cover, humidity, topography, and aspect (Hock, 1999, 2005; Pellicciotti et al., 2005; Sicart et al., 2008; Huss et al., However, it remains the most feasible approach to estimate melt in poorly instrumented watersheds given its simplicity and limited field data requirement compared to an energy balance approach (Hock, 2005; Fernández and Mark, 2016; Reveillet et al., 2017). The~~ melt simulated with the temperature index model was added to the precipitation amount for the Flux-PIHM forcing inputs.

10   We used the PIHMgis software (Bhatt et al., 2014) to construct an unstructured domain of 188 cells over the Gavilan Machay subcatchment using a 30 m resolution Shuttle Radar Topography Mission (SRTM) Digital Elevation Model (DEM) (Farr et al., 2007). Although a major feature of PIHMgis is its tight integration with spatial and temporal datasets for model inputs such as soil properties and meteorological forcing, these datasets only cover densely monitored regions, mostly within North America and Europe. For meteorological forcing, we used ~~spatially distributed temperature, precipitation and relative humidity measured~~

15 ~~and interpolated in the watershed, along with incoming shortwave and longwave radiation, wind speed, and air pressure obtained from the corresponding GLDAS grid cell~~ the spatially distributed inputs described in Section 3.1. Vegetation mapping by McLaughlin (2017), based on 30-cm resolution aerial photo surveys conducted by the Sistema Nacional de Información de Tierras Rurales e Infrastructura Tecnológica (SIGTIERRAS; http://www.sigtierras.gob.ec/descargas/), provided land-cover types and boundaries. Built-in land-cover parameters from Noah-LSM were used for the "grassland/herbaceous" type at low-

20 est elevations corresponding to páramo, the "barren/sparsely vegetated" type for intermediate elevations with rock/dirt/gravel, and the "perennial ice/snow" type for the ice-covered areas. This approach simplifies the mix of tussock grasses, acaulescent rosettes, and cushion plants that make up the páramo into a single representative "grassland/herbaceous" type in order to reduce the calibration burden. For the grassland/herbaceous land cover type, the default monthly Leaf Area Index (LAI) values were replaced with measurements from MODIS (Vermote, 2015) to avoid using incorrect seasonal changes from the original

25 model settings for this tropical region. Hydraulic parameters were manually calibrated to match observed discharge at Gavilan Machay.

4   Results and Discussion

This section presents the respective insights gained from each of the three methods on the temporal relationship among meltwater, groundwater, and discharge: the mixing model analysis offers discrete multi-year estimates over five years, the time

30 series analysis shows fine-scale hourly resolution correlations, and the integrated hydrological model explores intermediary weekly to seasonal processes within a one-year simulation period containing a strong El Niño event. A complete interpretation of the multi-scale temporal variabilities and their hydroclimatic controls emerges in Section 4.3.2 when evaluating the model simulations in relation to the mixing model and time series analysis results.

4.1 Mixing-model analysis of meltwater contributions to discharge

Total cation concentrations provide a summary representation of hydrochemistry results from the five dry-season synoptic sampling periods in Figure ~~2(a) and (c)~~3. These plots show that even though hydrochemical conditions vary over the different periods, groundwater samples, which geochemically interact with soil and rocks, consistently contain much higher ion concentrations than meltwater samples~~, which are relatively solute-free~~. The distinctive chemistries of groundwater and meltwater make it possible to use the mixing model approach to estimate their relative contributions to streamwater, which shows an increase in ion concentration while moving downgradient due to the cumulative addition of groundwater (see Figure 1(b) for sample locations). ~~Bivariate plots of specific hydrochemical constituents (~~We chose as tracers those analytes that most consistently showed the mixed sample visually falling close to the line between its two source samples in the bivariate plots in Figures S4-S8~~) support the selection of the following potential tracers~~: sum of monovalent cations, Mg^{2+}, Ca^{2+}, Cl^-, and HCO_3^-. Hierarchical cluster analysis lends confidence that these five potential tracers can be used in the mixing model analysis to distinguish between groundwater and melt samples as different watershed-level end-members (Figure S9). Precipitation was not included as an end-member, because precipitation samples tended to plot outside the range of stream samples bracketed tightly by groundwater and meltwater samples in bivariate plots. Rather than directly add to streamflow, any precipitation that fell close to the sampling time likely evapotranspired or infiltrated and contributed to streamflow through groundwater.

HBCM results in Figure 4 illustrate the importance of both meltwater and groundwater in the watershed. Surficial meltwater comprises between 23-66% of discharge during the five dry-season sampling periods, with groundwater constituting the remaining 34-77% at any given time. Notable differences were observed across the sampling periods. The higher ~~melt fraction~~ relative melt contribution during February 2017 compared to January 2012 could reflect the accelerating melt rates observed on Chimborazo (La Frenierre and Mark, 2017). However, the absolute melt contribution, determined by applying estimates of ~~melt fractions~~ relative melt contributions to average observed weekly discharge measurements around the sampling time, was in fact lowest in February 2017, because of significantly less ~~groundwater~~ total discharge compared to the other sampling periods (Figure 4(b)). The lower total discharge was likely due to lower precipitation and temperature during the weeks around the sampling period compared to during the other sampling periods (Figure S1). Our findings across the five sampling periods demonstrate that one single synoptic tracer test should not be directly generalized or interpreted without considering temporal dynamics and groundwater conditions.

~~Across all sampling periods, the groundwater fraction in the Gavilan Machay discharge appears high~~Our results show Volcán Chimborazo to deviate from trends found at the well-studied Cordillera Blanca, likely due to its distinct climatic and geologic conditions. When compared to an exponential fit between relative groundwater contribution and glacierized fraction for four watersheds in the Cordillera Blanca (Baraer et al., 2015), our ~~HBCM-derived estimates~~ estimates for groundwater contributions in Gavilan Machay are approximately twice as large. ~~Furthermore, previous studies in the Cordillera Blanca found greater specific discharge in more highly glacierized areas (Baraer et al., 2009; Mark and Seltzer, 2003). In contrast, when we extended our HBCM analysis downgradient to the Boca Toma diversion point, results suggest that~~ Also, the glacierized Gavilan Machay sub-catchment of the Upper Río Mocha watershed has a specific discharge that is less than half of that in the non-glaciated
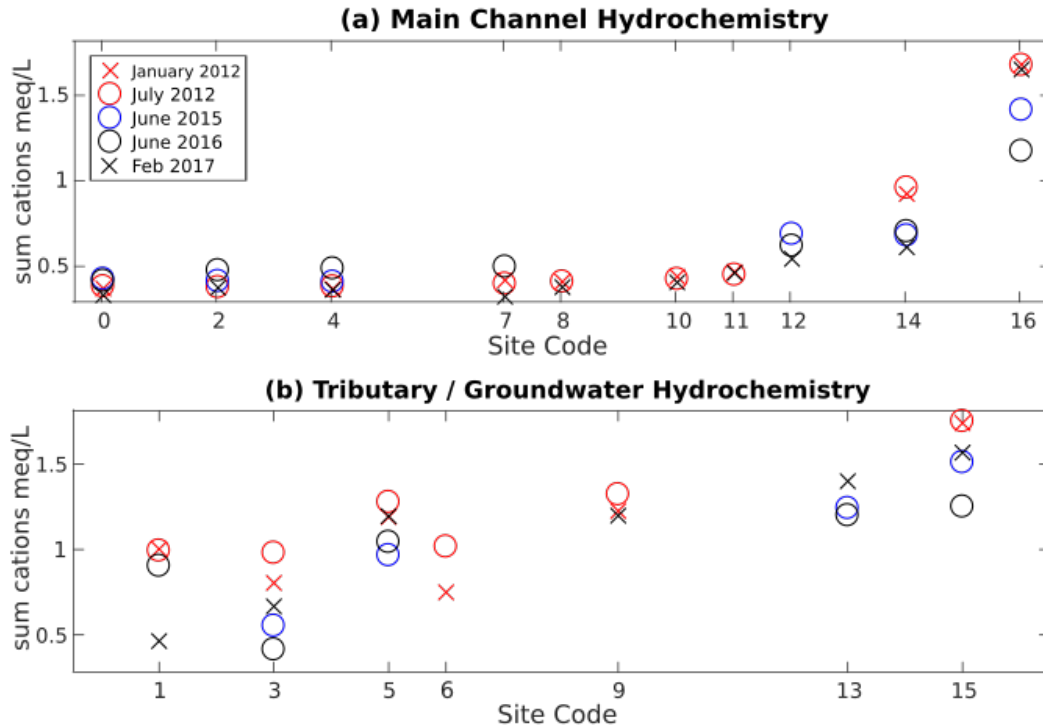
Figure 3. (a) Hydrochemistry at different sampling locations along the Gavilan Machay main channel shows variability in space and over the five sampling periods; site codes are ordered from highest (0 for meltwater) to lowest (16 for Boca Toma) elevation (see Figure 1(b)). **(b)** Hydrochemistry for different tributary (sites 3, 6, 9, and 15) and groundwater (spring) samples (sites 5 and 13), ordered from highest to lowest elevation, show variability in space and time.

portion~~of the Upper Río Mocha watershed. Wetter inner tropics climate and volcanic subsurface properties likely contribute to the distinct findings on Volcán Chimborazo~~, in contrast to the greater specific discharge generally found with greater glacierized areas in the Cordillera Blanca (Baraer et al., 2009; Mark and Seltzer, 2003).

HBCM implementation with five different field campaigns enabled us to evaluate uncertainties due to distinct sampling plans (details in Supplementary Information - Table S1). We found that changing HBCM cell configurations could generate up to a 23% melt fraction difference in estimates. Also, having fewer HBCM analysis cells (e.g., longer stream reaches) and fewer groundwater samples consistently led to greater HBCM residual errors. Too few groundwater samples becomes problematic when groundwater is not a homogeneous end-member throughout the watershed, which ~~can be seen to be~~ is the case in Gavilan Machay~~from Figure 2(c), which shows spring samples containing~~, which contains springs with somewhat higher solute concentrations at lower elevations (Figure 3(b)). Further, ~~groundwater end-member errors~~ errors in the estimated groundwater contribution grow when using fewer and longer reach cells, ~~while~~ because with additional and shorter reach cells, observations can reset the stream channel chemistry to correct concentrations. These results demonstrate the importance of
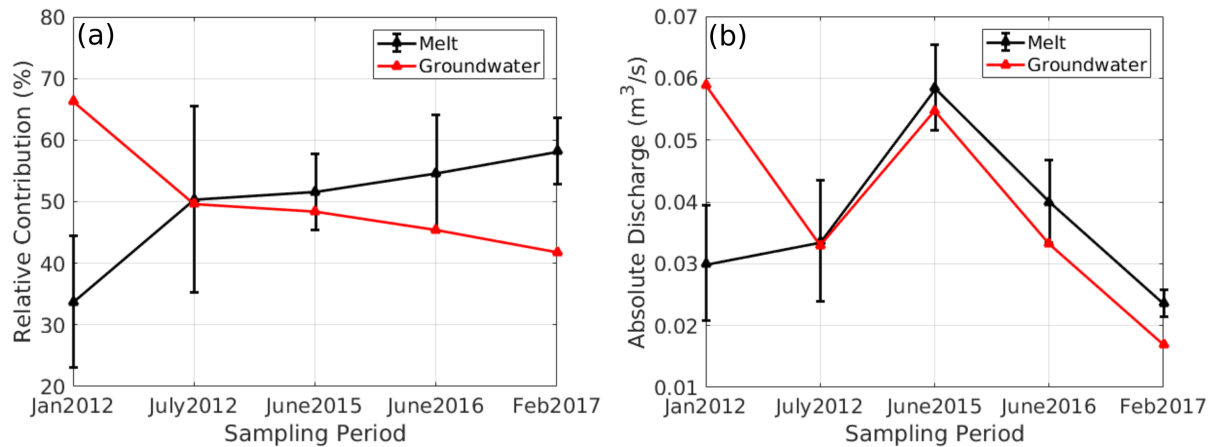
Figure 4. The HBCM mixing model predicts a range in relative ~~surficial~~ meltwater contributions to discharge over five discrete sampling times, which may reflect both temporal changes and uncertainties. Error bars bracket HBCM estimates that produced similar best matches to observed tracer concentrations; however, actual ~~uncertainty~~ uncertainties are ~~much~~ higher because of ~~the~~ residual errors. Absolute meltwater discharge contributions can vary in time very differently than relative inputs, in part due to varying groundwater contributions.

adequately measuring the spatial variability of the surface and subsurface flow network, and they prompt the use of alternative methods to help constrain uncertainties in HBCM analysis results.

4.2 Time series and spectral analysis of hydroclimatic controls

Because of the uncertainties and long time gaps in the HBCM analyses, we applied ~~time series analysis~~ statistical analyses to the
5   continuous data available from July 2015 to March 2016 at the Boca Toma weather station and Gavilan Machay gauging station to further infer characteristic trends between ~~glacial melt~~ meltwater and discharge and their climatic controls. Considering air temperature as a proxy indicator of ~~glacial~~ meltwater, the hourly cross correlation of air temperature leading discharge at Gavilan Machay in Figure 5(a) shows a strong diurnal signal, with peak discharge occurring four hours after the warmest part of the day at an average rate (0.1 m^3/s) that is about twice the magnitude of average morning discharge.
10   To determine if melt could be driving discharge variability beyond diurnal time scales, we examined the ~~spectral~~ magnitude squared coherence between temperature and discharge in Figure 5(c), which quantifies their correlation at a certain ~~time frequencies (or periods~~ period (inverse time-frequency). As expected from the time-series results, the most prominent feature is the peak at a period of 24 hours. Interestingly, the next highest coherence is at a period of 12 hours. While this could be a harmonic artifact of the dominant 24-hour trend, it is supported by a slight temperature increase commonly observed around
15   11pm~~, possibly due to adiabatic warming as downslope winds develop~~. The resulting increase in discharge, while detectable, is inconsequential to the total daily water balance. Other very narrow coherence peaks at periods less than 12 hours are likely spurious, because the power spectral densities of both temperature and discharge are low over that range (Figure S10). How-

14
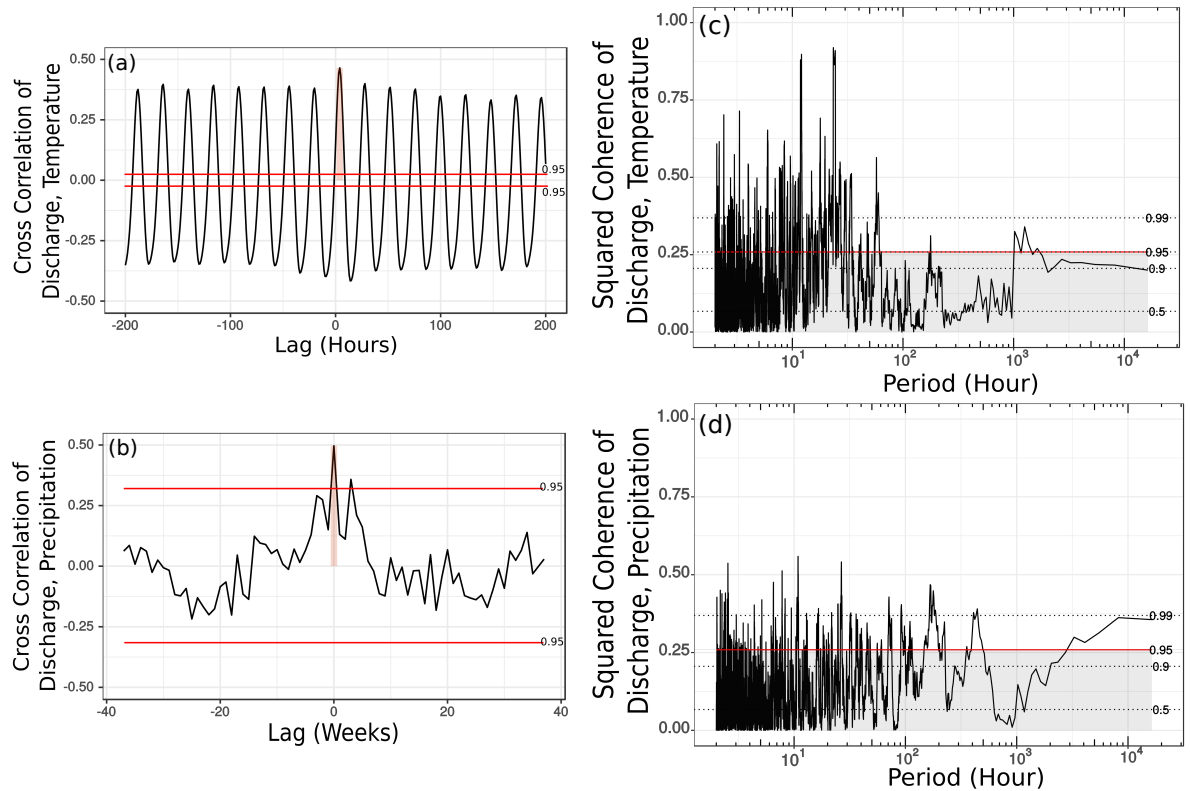
Figure 5. Cross-correlations (with 95% confidence interval shown) of observed discharge at Gavilan Machay with **(a)** hourly temperature and **(b)** weekly precipitation show that discharge has a clear diurnal link with temperature at about a 4 hour lag and a strong relationship with weekly precipitation, respectively. ~~Spectral~~ Magnitude squared coherence (with various confidence intervals shown) between discharge and **(c)** temperature exhibits a high peak at 24 hours corresponding to the cross-correlation result, as well as a strong peak at 12 hours, and a more moderate ~~peaks~~ peak at a multi-day ~~scales~~ scale. The coherence between discharge and **(d)** precipitation peaks between 100 to 200 hours (about 1 week) and may also be significant at scales approaching one year.

ever, the smaller but broader peak around 50 to 60 hours suggests that multi-day warming may also drive multi-day discharge events, though this link is much weaker than the diurnal response.

The substantial groundwater contributions to discharge inferred from the HBCM analysis prompts a look at not only melt but also precipitation controls on multi-day discharge. Hourly precipitation and discharge are very weakly correlated (Figure

5   S11(a)); however, a ~~correlation of r_{xy} =~~ significant correlation of 0.5 appears for weekly averages with zero time lag (Figure 5(b)). Correspondingly, a high (above 95% confidence interval) and broad coherence peak between precipitation and discharge can be seen over periods of about one week (168 hours) (Figure 5(d)). Together, these results suggest that sustained rain events influence discharge over a week, and therefore that rainwater tends to infiltrate instead of flow quickly overland. Other

15

statistically significant (at the 95% confidence interval) coherences between discharge and both temperature and precipitation across multi-week to multi-month periods further support ~~slow~~ the role of even slower subsurface flow pathways.

Combining the time series analysis with the HBCM results suggests that streamflow at Gavilan Machay is heavily influenced by both surficial meltwater and groundwater, and that the latter is driven by precipitation. Furthermore, time series and spectral analyses highlight temporal links not easily found through a fieldwork-intensive tracer-based approach: meltwater feeds discharge at Gavilan Machay on an hourly time scale, while weekly discharge responds most strongly to precipitation events. There are, however, limitations to this statistical assessment that result from the short nine-month dataset, which precludes robust examination of any seasonal to multi-year responses to bimodal wet and dry seasons and El Niño effects. Hydrologic modeling in the following section can address this, as well as questions about ~~detailed physical processes, such as quantifying how much~~ the quantitative role of melt contributions or groundwater ~~may buffer~~ buffering periods of low rainfall.

4.3 Integrated Hydrologic Model Simulations

4.3.1 Calibration Results

Matching the observed discharge dynamics with the hydrologic model required calibration of two different melt factors based on time period: a lower value of 7.10 mm.w.e. (millimeters water equivalent) C^{-1} day^{-1} over December 2015-February 2016 and a higher value of 8.64 mm.we.°C^{-1} day^{-1} over the rest of the simulation. The estimated melt factors fall within the range of melt factors calculated for other glaciers in the tropics (3.5-9.9 mm.we.°C^{-1} day^{-1}) reported in Fernández and Mark (2016). Our simulation period coincides with a strong El Niño event that generated the warmest and driest conditions from late November 2015 to the start of February 2016 (Figure 6(a)–(b)). The lower melt factor at this time dampens the intensity of glacier melt, possibly because of the absence of heat transfer from rain (Francou, 2004), but it nonetheless simulates among the highest glacier melt volumes of the simulation period (Figure 6(a)), consistent with other studies showing increased glacier melt in response to El Niño events in the Andes (Francou, 2004; Veettil et al., 2014a; Manciati et al., 2014; Maussion et al., 2015; Veettil et al., 2016). Huss et al. (2009) similarly estimated a lower melt factor in the Swiss Alps ~~when air temperature was high in response to longwave~~ under warmer conditions, which they attributed to warmer conditions being driven by longwave rather than shortwave radiation. Overall, in Gavilan Machay, the average specific glacier melt rate (in water equivalence) simulated over glaciated areas below the ELA was 1.5 m/yr. This falls within the range measured at the Reschreiter Glacier tongue, bracketed by ~~geodetic~~ mass balance estimates on slower-melting debris-covered ice of 0.87 m/yr (1997–2013) and 0.54 m/yr (June 2012–January 2013), and average ablation stake observations on faster-melting clean ice of 3.4 m/yr (June–November 2016). Although useful for comparing against the calibrated melt model, these measurements do not cover sufficient areas and periods of time to constrain separate melt factors for debris-covered and clean-ice melt factors.

Over the entire watershed, the resulting calibrated glacier melt production is equivalent to 68% of the precipitation input and 567% of the simulated snowmelt amount during the simulation period. Based on temperature, Flux-PIHM partitioned the precipitation input into 12% snowmelt and 88% rainfall. The much smaller amount of simulated snowmelt compared to glacier melt supports the earlier suggestion (Section 3.3) that snowmelt could be precipitation-limited rather than energy-limited. This

helps justify our separate approach of simulating snowmelt through Flux-PIHM's energy balance module while simulating glacier melt through a calibrated temperature-index model, because energy balance calculations of glacier melt would be much more sensitive to uncertainties in coarse-scale radiation inputs than snowmelt. We do acknowledge, however, that snowmelt simulations depend on lapse-rate-determined precipitation inputs that have their own uncertainties (Section 3), and so our

5 calibrated glacier melt may include some amount of snowmelt that is not represented in the model.

The calibration procedure also involved soil parameter adjustments. Hydraulic parameter estimates in páramo environments are scarce, and their characterization can be uncertain (Buytaert et al., 2006). For an initial estimate, we applied pedotransfer functions used in Flux-PIHM (Wosten et al., 1999) to a range of páramo soil measurements from a study area 20 km northwest of Chimborazo (3800 to 4200 m.a.s.l.) (Podwojewski et al., 2002) and from a study watershed on glaciated Volcán Antisana

10 also in the Ecuadorian Andes (4000-4600 m.a.s.l.) (Minaya, 2016) (see ~~supplementary information – Table S2 –~~ Table S2 for full details). We then calibrated the model for three mapped land-cover zones corresponding to páramo, rock/dirt/gravel, and ice (Figure 1). In the páramo zone (Table 1), matching observed discharge required lower hydraulic conductivity and greater water retention (expressed in van Genuchten hydraulic parameters) than initially estimated. This is likely due to high organic matter content supported by the study area's sub-humid conditions and the well-recognized retentive hydraulic properties of

15 páramo soils (Podwojewski et al., 2002; Buytaert et al., 2006). In the sparsely vegetated and ice-covered zones, the calibration yielded higher hydraulic conductivities and lower water retentions than in the páramo zone, corresponding to reduced organic matter fraction and fractured bedrock, though the hydraulic conductivities were still lower than the initial estimates from the pedotransfer functions.

Simulation results in Figure 6(c) show that the calibrated model parameters closely produced the observed weekly discharge,

20 including lower discharge under the drier and warmer El Niño conditions in December 2015-January 2016. The single major model mismatch occurred at a precipitation-driven discharge peak in February 2016. This could reflect uncertainties from the soil parameter calibration, as well as from our use of a lapse rate-based precipitation field over complex terrain, in which high-altitude precipitation events may not all be recorded at the low-altitude rain gauge. On shorter timescales, hour-of-day simulation results in Figure 7(b) demonstrate that the model does produce a diurnal trend, but with slightly less than half the

25 average range and at a 6-hour later peak compared to observations (Figure 7(a)). These hourly discrepancies can be attributed to weaknesses in the simple melt model. Hock (2005) argued that ~~TI~~ temperature index models can successfully capture seasonal glacier melt trends but struggle with diurnal fluctuations, which are strongly driven by solar radiation dynamics. Although our simulations cannot reliably produce the timing of hourly discharge, they can provide informative lower bounds on the size of the average diurnal range.

17
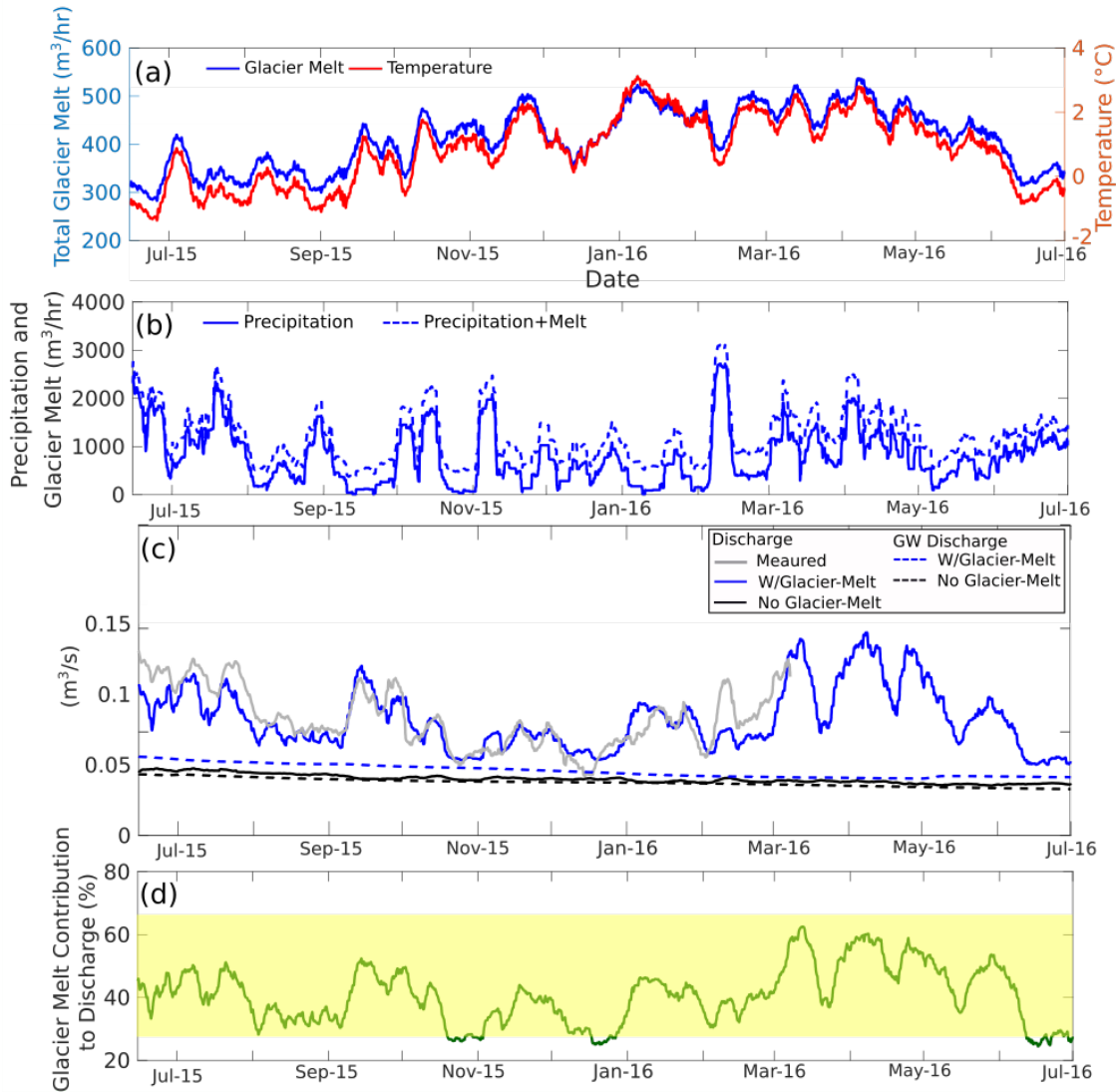
Figure 6. Time series of weekly moving average of **(a)** average air temperature <u>over the ablation zone (glacier-covered areas</u> below <u>the</u> ELA (5050 m.a.s.l.)~~and over glaciers~~<u>)</u> and simulated <u>glacier</u> melt ~~inputs~~<u>production</u>; **(b)** precipitation (solid line), and precipitation+<u>glacier</u> melt (dashed lines) ~~) inputs~~ <u>production</u> **(c)** discharge at Gavilan Machay from observations (gray), calibrated simulations (blue solid), and simulations with no ice-melt (black solid); groundwater ~~distribution~~ <u>contribution</u> to discharge for calibrated (blue dashed) and for no-ice simulations (black dashed); and **(d)** simulated percent <u>glacier</u> melt contribution to discharge at Gavilan Machay. <u>The shaded block shows the range of percent melt contributions estimated for five sampling periods over 2012-2017 from the mixing model; these estimates may include snowmelt in addition to glacier melt, but omit meltwater contributions through groundwater.</u>

18

	KINF (m/s)	KSATV (m/s)	KSATH (m/s)	Porosity	Residual Moisture	α (1/m)	β (-)
Range predicted for observed páramo soil textures*	3.71E-8–8.28E-5	8.42E-8–3.71E-5	8.42E-7–6.96E-5	0.418–0.493	0.05	0.327–5.82	1.1–1.173
Calibrated: Grassland$^\diamond$	1.23E-07	4.02E-08	4.02E-07	0.458	0.05	0.488	1.066
Calibrated: Sparsely vegetated$^\diamond$	1.43E-07	4.63E-08	4.63E-07	0.459	0.05	0.585	1.063
Calibrated: Ice-covered$^\diamond$	2.07E-07	6.71E-08	6.71E-07	0.461	0.05	0.863	1.06

*Predicted using pedotransfer functions with 9 páramo soil texture measurements from Ecuador. Samples are from 3 locations in a glaciated watershed in Volcan Antisana (Minaya, 2016) and 4 locations about 20 km northwest of Chimborazo (Podwojewski et al., 2002) (see Supplementary Information for more details).

$^\diamond$Calibrated to match observed discharge at Gavilan Machay

Table 1. Soil hydraulic parameters calibrated for the three soil type areas compared against the range predicted using the pedotransfer function with measured páramo soil textures in Ecuador (Podwojewski et al., 2002; Minaya, 2016). Parameters include hydraulic conductivities for vertical infiltration (KINFV), vertical ~~unsaturated~~ saturated zone flow (KSATV), and horizontal saturated zone flow (KSATH); porosity~~(SMCMAX)~~; residual soil moisture~~(SMCMIN)~~; and shape parameters (α and β) for the van Genuchten moisture retention curve: ~~$\theta = \theta_{res} + porosity \times \left(\frac{1}{1+abs(\alpha \times \psi)}\right)^{\beta}\right)^{(1-\frac{1}{\beta})}$~~ $\theta = \theta_{res} + porosity \times \left(\frac{1}{1+|\alpha\psi|^{\beta}}\right)^{(1-\frac{1}{\beta})}$, with water content θ and pressure head ψ.

4.3.2 Simulations of relative glacier melt contribution to discharge

To quantify relative glacial meltwater contribution to stream discharge using Flux-PIHM, we compared the calibrated discharge simulations at Gavilan Machay (Q_{Calib}) with simulations that omitted glacier meltwater in the forcing inputs (~~Q_{NoMelt}~~$Q_{NoGlacierMelt}$). We then calculated relative glacial meltwater contribution to discharge via:

$$\%\underline{MeltGlacierMelt} = \frac{Q_{Calib} - Q_{NoMelt}}{Q_{Calib}}\frac{Q_{Calib} - Q_{NoGlacierMelt}}{Q_{Calib}} \times 100\%. \tag{3}$$

~~This estimate represents the additional discharge due~~ Apart from the addition of glacier melt in the calibrated case, the two model scenarios include the same model inputs, including air temperature, precipitation (including identical snowmelt), land cover, and hydrologic properties. Thus, our calculation of change between the two scenarios isolates the effect of having glacier melt versus not having glacier melt. Overall, over the one-year simulation period, an average 52% of stream discharge in Gavilan Machay can be attributed to glacier melt, ~~but~~ compared to an 8% contribution by snowmelt. Because the simulated glacier melt amount was calibrated in addition to precipitation inputs, we consider this glacier melt contribution to originate from the pre-existing ice reservoir at the start of the model period. However, as noted above (Section 4.3.1), the calibrated
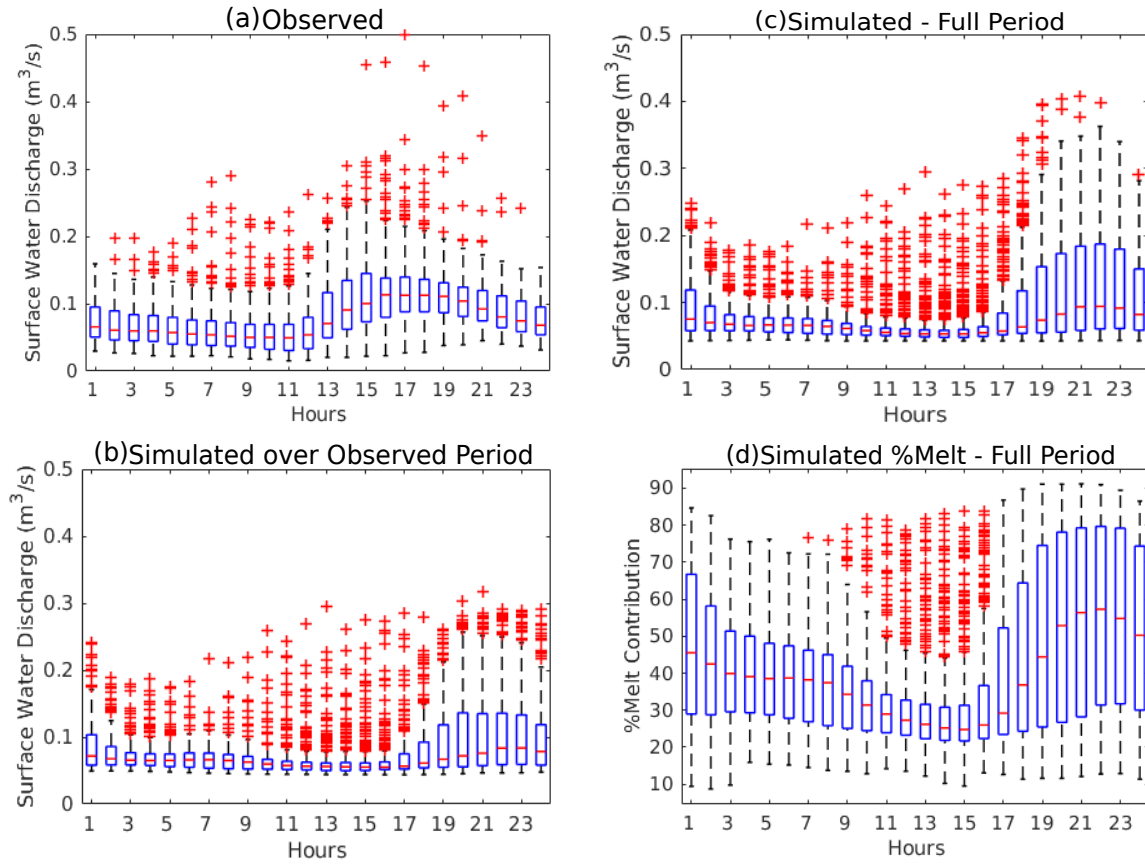
Figure 7. Box plots over local hour-of-day showing 25 – 75 percentiles with boxes and maximum and minimum with whiskers for **(a)** observed discharge over the 9-month observation period, **(b)** simulated discharge over the 9-month observation period, **(c)** simulated discharge over the 12-month simulation period, and **(d)** simulated percent glacier melt contribution to discharge over the 12-month period. Simulations do capture diurnal patterns, but with an underestimated magnitude and shifted peak. Simulated percent glacier melt contributions to discharge closely mirror the simulated diurnal fluctuations in discharge.

glacier melt contribution could include some amount of snowmelt not fully accounted for in the model due to uncertainties in precipitation inputs.

The estimate provided by equation (3) may not exactly correspond to ~~HBCM results~~ the HBCM result for meltwater contribution for a number of reasons. First, the water balance impact of glacier melt conveyed in equation (3) may not equal the proportion of meltwater in a sample of discharge water if, for example, melt inputs facilitate more runoff of precipitation-sourced water. Also, while equation (3) ~~isolates just the effect of glacier melt~~ aims to isolate glacier melt of pre-existing glacier ice, HBCM estimates could include ~~snow-melt~~ snowmelt and melt of freshly accumulated ice, depending on the composition of the meltwater sample taken just below the glacier tongue. Lastly, any melt that infiltrates is considered as part of the ground-

5

20

water rather than melt ~~fraction~~ contribution in HBCM estimates, while equation (3) includes the effect of both surficial and groundwater contributions of meltwater to discharge.

These conceptual discrepancies complicate comparisons between the two methods, but it is possible to assess the June 20-25, 2016 HBCM result against the simulation (other HBCM periods fall outside the one-year model period). During June 20-25, 2016, the 45-64% estimate with HBCM is higher than the average simulated relative melt contribution of 29%, but it falls within the simulated hourly range of 13-70% over that time. Considering that samples were collected during the daytime when melt contributions were generally high, the results from these two approaches reasonably agree.

While process-driven temporal patterns were difficult to glean from the sparsely spaced and uncertain HBCM results, Flux-PIHM simulations in Figure 6(d) clearly indicate considerable variability in weekly glacier melt contributions of 25–61% over June 2015–June 2016. This range compares very closely with the 23–66% range bounded by the five HBCM estimates spanning January 2012 to February 2017 (indicated by the shading in Figure 6(d)), lending further confidence in the consistency between the watershed and mixing model results, despite the differences in temporal and other types of representation noted above. Hourly distributions of simulated glacier melt contribution in Figure 7(d) show an average diurnal range of 25-68%; given that the actual range is likely even broader due to underestimations by the temperature index model, diurnal fluctuations in relative melt contributions may be of similar or even greater magnitude than changes on weekly to monthly timescales.

Comparing Figures 6(c) and (d) reveals a remarkably strong correlation (0.89) between simulated weekly discharge and relative glacier melt contributions, indicating that major discharge peaks over multi-day timescales are melt-driven, a time-scale link that was masked in the time series analysis in Section 4.2 by the overwhelming diurnal signal between temperature and discharge. Figure 8(~~a~~b) shows strong coherence over 30 to 80 day periods between simulated ~~melt inputs and relative~~ glacier melt production and relative glacier melt contributions to discharge, highlighting those timescales as the most prominent ~~beyond diurnal correlations. Most~~ for direct glacier melt inputs beyond diurnal time scales. Although occurring at a longer multi-month timescale, these melt contributions to discharge nonetheless appear to happen mostly through fast surface runoff; the model showed most (86%) of the glacier melt contribution to discharge ~~occurred~~ occurring through surface runoff processes~~in the model~~, consistent with the hourly correlations found between observed discharge and temperature in Section 4.2. With the model, the influence of ~~melt~~ glacier melt production on discharge is clear during times such as early January 2016, when an uptick in discharge occurs despite low precipitation, due to warm temperatures and greater melt production and contribution (Figure 6).

~~Interestingly~~Unexpectedly, the peak relative glacier melt contributions (Figure 6(d)) do not always align with glacier melt production patterns (Figure 6(a)) (e.g., in early February 2017, percent glacier melt contribution peaks just when temperature and ~~melt inputs~~ glacier melt production dip), and their weekly correlation is not strong at a 95% confidence level (Figure S11(b)). Squared coherences in Figure 8(a) indicate that this is because relative glacier melt contribution also responds to precipitation~~inputs~~, and this happens at weekly and multi-month timescales when correlations with ~~melt inputs~~ glacier melt production are low (Figure 8(b)). In fact, the strong coherence between precipitation and glacier melt contribution around 6 to 14 day periods reveals that the high correlation between observed weekly precipitation and discharge in Section 4.3 relates to glacier melt contributions. Inspection of time periods such as mid-February and the start of April 2016 ~~(Figure 6)~~ show
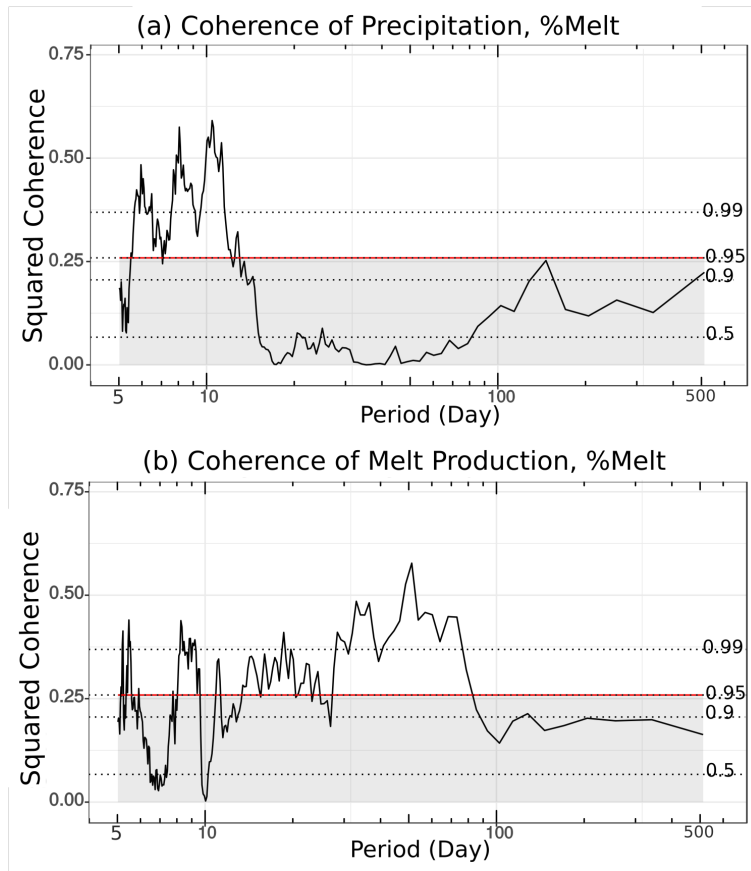
Figure 8. ~~Coherences~~ Magnitude squared coherences between simulated percent glacier melt contribution to discharge with **(a)** precipitation and **(b)** simulated glacier melt ~~input~~production. Calculations used daily average data to avoid known uncertainties in modeling diurnal fluctuations of glacier melt production. Precipitation and glacier melt ~~inputs~~ production appear to be related to glacier melt contributions at complementary timescales.

that rainy periods can augment ~~melt inputs~~glacier melt contributions to discharge (Figure 6(b), (d)) . During those times, increases in relative glacier melt contributions to discharge coincided with precipitation events during local drops in ~~melt input~~ ~~(Figure 6)~~glacier melt production, possibly because ~~weeklong~~ week-long precipitation creates antecedent moisture conditions that enhance the fraction of glacier meltwater that runs off over the surface. Surface runoff can be expected to contain mostly glacier meltwater or high-elevation precipitation, because runoff generally does not occur on low-elevation páramo soils except under intense precipitation (Sarmiento, 2000; Harden, 2004).

At greater timescales, significant coherences between precipitation and simulated relative glacier melt contributions around 120+ days (Figure 8(a)) correspond to overall lowest relative glacier melt contributions during the dry El Niño period (December 2015-February 2016) and highest relative contributions during the two wet seasons (February-May and October-November)~~. These~~, possibly due to a transfer of heat from rain to ice. These glacier melt contribution responses to bi-seasonal

22

to interannual climatic patterns likely occur through slower groundwater pathways; the simulation with glacier melt produces 18% greater groundwater contributions to discharge than that without glacier melt (Figure 6(c)). This supports the hypothesis that some amount of glacier meltwater infiltrates and recharges to groundwater that then discharges farther downgradient to the stream channel. It should be noted, however, that the subsurface component of Flux-PIHM contains only a single shallow saturated zone, which mostly closely corresponds to a perched water table in the soil zone. This model implementation may not accurately represent additional deeper fractured bedrock aquifers systems, which could discharge groundwater to streams over shorter, multi-month time scales (Andermann et al., 2012), in contrast to the relatively constant groundwater dynamics simulated in Figure 6(c).

Our results may be particular to the more moist climate in the Gavilan Machay watershed, which supports constant groundwater discharge to the stream throughout the year and reflects compounded effects of melt inputs and rainfall conditions. However, although glacier melt intensifies discharge variability in this watershed, a baseline 25% glacier melt contribution throughout the simulation period indicates that a constant minimum level of glacier melt helps prevent episodes of even more extreme low flows during drought times, such as during El Niño conditions. Overall, an average 52% of discharge can be attributed to melt inputs over the model simulation test period.

5   Summary and Conclusions

Although meltwater is typically credited with modulating stream discharge by buffering periods of low precipitation, we demonstrate using a combination of methods that relative meltwater contributions may drive nearly all the variability in discharge (correlation of 0.89) over a range of hourly to multi-year timescales while buffering only against extreme low discharge periods in a humid glacierized watershed in the Ecuadorian Andes. Hydrochemical mixing model results for five sampling periods spanning 2012-2017 showed the meltwater fraction in discharge may have varied over approximately 20–65%. Hydrologic model simulations over June 2015–June 2016 produced a nearly identical range for weekly contributions. The model also predicted a very similar average diurnal range, which likely provided a lower bound of actual variability based on hydroclimatic data. This multi-scale variability in melt contributions can be attributed to dynamic climate forcings that also contain a range of temporal patterns (Figure 9). We found a strong correlation between diurnal temperature and discharge changes that likely reflects melt inputs production and supports the use of a temperature index melt model (Figure 9(a)). Although such a simple melt approach somewhat underestimated hourly fluctuation extremes with a lag, it led to reasonable weekly discharge predictions when implemented with a seasonally variable melt factor that possibly accounts for additional heat transfer from rainfall to ice during wet seasons. The hydrologic model Spectral coherence analysis of the model results showed that not only were diurnal discharge patterns responding to radiation-driven melt inputs melt production, but relative melt contribution and discharge variations over 30-80 day periods were also controlled by melt inputs controlled by extended glacier melt production periods that also contribute to discharge through surface runoff (Figure 9(c)).

Unexpectedly, model results showed that precipitation also boosted melt contributions to discharge, but on weekly and semi-annual timescales that complement the hourly and monthly timescales controlled by temperature and melt inputs production.
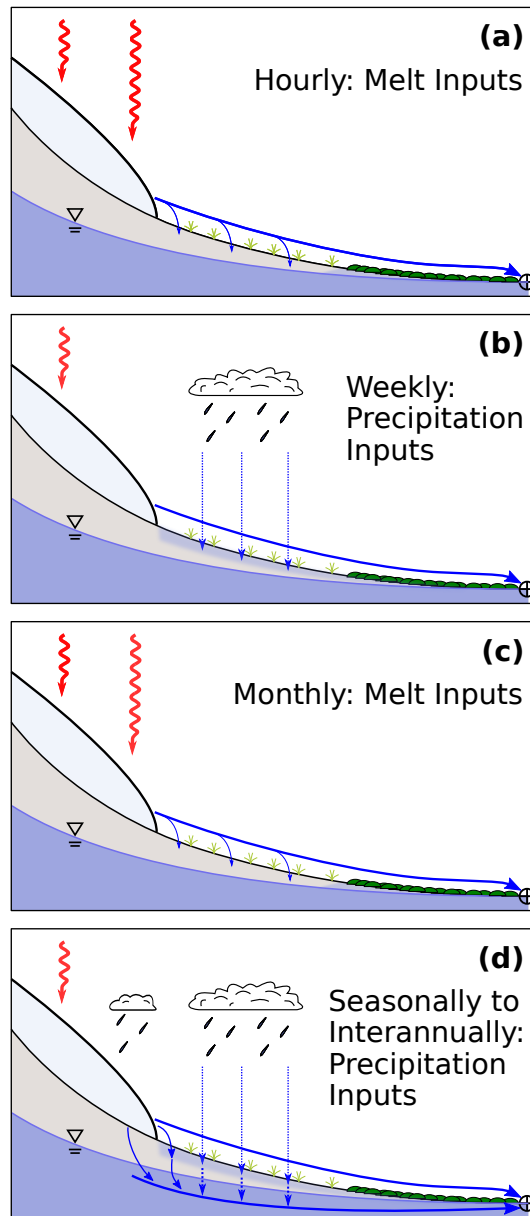
Figure 9. Relative melt contributions drive nearly all the variability in discharge in Gavilan Machay, mostly through surface runoff of glacial meltwater. What drives the variability in relative melt contributions to discharge? Our results show that this depends on the timescale. **(a)** Hourly timescale variability is controlled by radiation-driven (red arrows) melt ~~inputs at the glacier tongue~~ production (light blue slab at upper left), which readily runs off overland (thick blue arrow) and eventually reaches the watershed's discharge point (circle with cross). **(b)** Weekly timescale variability is controlled by weekly precipitation events, which likely generate antecedent moisture conditions (light blue shading) that promote greater meltwater runoff. **(c)** Monthly timescale variability is driven by monthly trends in melt generation, which contributes to discharge mostly through surface runoff. **(d)** Seasonal to interannual variability is driven by long-term precipitation, which can enhance melt by transferring heat from rain (blue arrows right of glacier tongue), and augment subsurface melt contributions through increased groundwater flow (thick blue arrow below water table).

Weekly precipitation events likely generate antecedent wet conditions that facilitate greater amounts of meltwater runoff (Figure 9(b)), while longer-term precipitation patterns appear to drive slow changes in melt additions to groundwater (Figure 9(d)). Most (86%) melt contributions to discharge occurred through surface runoff in the model, but some meltwater recharged to groundwater, ~~supporting~~ helping to support a relatively steady groundwater discharge to the stream that is about 18% greater

5 ~~than in the scenario without~~ with glacier melt than without glacier melt. As expected, strong El Niño conditions corresponded to some of the highest simulated melt inputs, but less easy to predict was that Gavilan Machay exhibited its lowest discharge during this time. Melt prevented streamflow from dropping below a baseline level during the warm and dry El Niño event, but discharge was much higher during wetter periods, in part because of the rainfall-enhanced melt contributions described above.

In glacierized watersheds, slower glacier melt contributions through groundwater are poorly constrained. Past studies have

10 identified a component of meltwater in the groundwater (Favier et al., 2008a; Lowry et al., 2010; Baraer et al., 2015; Minaya, 2016; Harrin but to our knowledge, our work is the first to quantify this component. Generally, fractured young volcanic bedrock systems can support extensive groundwater (Tague et al., 2008; Frisbee et al., 2011; Markovich et al., 2016) and may contain similar meltwater fractions as found here. However, meltwater-groundwater interactions may be more ubiquitous. Prominent groundwater pathways have also been identified in fractured crystalline bedrock (Tague and Grant, 2009; Andermann et al., 2012; Pohl et al., 2015),

15 morainic deposits (Favier et al., 2008a; Minaya, 2016; Somers et al., 2016), and alpine meadow soils (Loheide et al., 2009; Lowry et al., 20 Even in settings with limited groundwater networks, talus slopes and rock glaciers can serve as localized areas of meltwater recharge (Clow et al., 2003; Baraer et al., 2015; Harrington et al., 2018). More arid settings than the sub-humid Gavilan Machay could have a higher proportion of glacier melt in groundwater due to less precipitation inputs, but our results also indicate that precipitation may serve to enhance meltwater contributions.

20 The multiscale temporal variability of relative melt contributions to discharge has important implications for how to determine the hydrologic role of glaciers in watersheds, as well as for water resource management in fast-changing glacierized systems. Care must be taken in the implementation and interpretation of commonly employed tracer analyses. Potentially large diurnal fluctuations make it imperative to collect samples over consistent times of day, and weekly to interannual variability complicate extrapolations from single synoptic sampling estimates. Recharge ~~of meltwater~~ by glacier melt further confounds

25 the interpretation of groundwater as a source entirely distinct from surficial meltwater. These uncertainties, along with additional errors caused by heterogeneous groundwater chemistry and the choice of sample locations, limit the ability of tracer-based analyses to constrain dynamic melt contributions to discharge. Model simulations provide ideal temporal resolution, but they suffer from their own disadvantages~~. Easy to implement temperature-index models may not be reliable for predicting the full magnitude and timing of diurnal melt pulses, and they may require seasonal calibration of melt factors. Difficulties in~~

30 ~~obtaining soil and vegetation properties lead to further model errors~~, such as intensive data input requirements and uncertainties in parameter calibration.

For water resources, weekly to multi-year melt contributions to discharge are of greater interest than hourly fluctuations. At those timescales of concern, rain events and wet periods can accentuate relative melt contributions to streamflow in humid glacierized systems. This signifies a bonus in water yield, but it also intensifies discharge variability over weekly and seasonal

35 timescales, which can pose challenges if water storage infrastructure is unavailable. On an interannual basis, melt can augment

discharge during warm and dry El Niño events, but glacierized watersheds will likely experience greatest melt contributions during wetter times, when they are under the combined effects of enhanced ablation ~~and precipitation.~~ (due to transfer of heat from rain to ice) and antecedent moist conditions (due to precipitation). Looking at downstream implications, the small (7.5 km^2) Gavilan Machay headwater catchment contributes a range of only 9 to 26% of the discharge to the Boca Toma diversion point, which corresponds to surficial meltwater making up a range of just 4 to 15% of the water to the irrigation system, based on mixing model estimates. However, La Frenierre (2014) showed that farming communities cannot afford to lose any of the water; already, the irrigation system consistently fails to deliver its current allocations. Furthermore, if groundwater at Gavilan Machay also contains meltwater, as our simulations suggest, the actual total amount of meltwater contribution could be even higher than that estimated for surficial runoff of meltwater by the mixing model. Additional downstream monitoring would enable further extensions of the watershed model to investigate how meltwater contributions and temporal discharge variabilities found in Gavilan Machay propagate downgradient to successively larger watersheds, as non-glacier sourced groundwater contributions increase. Spatial patterns of groundwater contributions within Gavilan Machay reveal sharp increases where geologic features likely create localized discharge points (Figure S12). This indicates that extrapolations downstream will likely depend on geological conditions that control groundwater, in addition to watershed size and climate inputs.

In the future, should Reschreiter Glacier ~~melt~~ disappear completely, overall discharge in Gavilan Machay could decrease by ~~more than~~ up to about 50%, even if precipitation ~~remains adequate to maintain a~~ and temperature remain the same and relatively constant groundwater flow ~~. This suggests~~ continues. The exact decrease will depend on how much of our melt estimate may include contributions by snowmelt and melt from freshly accumulated ice that will persist as discharge sources. Overall, our findings suggest that in response to glacier loss in a warming climate, glacierized watersheds in the humid inner tropics may eventually experience steadier discharge, but potentially at significantly decreased rates.

5

References

Andermann, C., Longuevergne, L., Bonnet, S., Crave, A., Davy, P., and Gloaguen, R.: Impact of transient groundwater storage on the discharge of Himalayan rivers, Nature Geoscience, 5, 127–132, https://doi.org/10.1038/ngeo1356, 2012.

Andrews, E. D.: Measurement and computation of bed-material discharge in a shallow sand-bed stream, Muddy Creek, Wyoming, Water Resources Research, 17, 131–141, https://doi.org/10.1029/WR017i001p00131, 1981a.

Andrews, E. D.: Measurement and computation of bed-material discharge in a shallow sand-bed stream, Muddy Creek, Wyoming, Water Resources Research, 17, 131–141, https://doi.org/10.1029/WR017i001p00131, 1981b.

Baraer, M., McKenzie, J. M., Mark, B. G., Bury, J., and Knox, S.: Characterizing contributions of glacier melt and groundwater during the dry season in a poorly gauged catchment of the Cordillera Blanca (Peru), Advances in Geosciences, 22, 41–49, https://doi.org/10.5194/adgeo-22-41-2009, 2009.

Baraer, M., Mark, B. G., McKenzie, J. M., Condom, T., Bury, J., Huh, K.-I., Portocarrero, C., Gómez, J., and Rathay, S.: Glacier recession and water resources in Peru's Cordillera Blanca, Journal of Glaciology, 58, 134–150, https://doi.org/10.3189/2012JoG11J186, 2012.

Baraer, M., McKenzie, J., Mark, B. G., Gordon, R., Bury, J., Condom, T., Gomez, J., Knox, S., and Fortner, S. K.: Contribution of groundwater to the outflow from ungauged glacierized catchments: a multi-site study in the tropical Cordillera Blanca, Peru, Hydrological Processes, 29, 2561–2581, https://doi.org/10.1002/hyp.10386, 2015.

Barba, D., Samaniego, P., Eissen, J.-p., Robin, C., Fornari, M., Cotten, J., and Beate, B.: Geology and structure of the late Pleistocene to Holocene Chimborazo stratovolcano (Ecuador), 6th International Symposium on Andean Geodynamics (ISAG 2005, Barcelona), pp. 90–93, 2005.

Barnett, T. P., Adam, J. C., and Lettenmaier, D. P.: Potential impacts of a warming climate on water availability in snow-dominated regions, Nature, 438, 303–309, https://doi.org/10.1038/nature04141, 2005.

Bhatt, G., Kumar, M., and Duffy, C. J.: A tightly coupled GIS and distributed hydrologic modeling framework, Environmental Modelling & Software, 62, 70–84, https://doi.org/10.1016/j.envsoft.2014.08.003, 2014.

Bradley, R. S.: CLIMATE CHANGE: Threats to Water Supplies in the Tropical Andes, Science, 312, 1755–1756, https://doi.org/10.1126/science.1128087, 2006.

Bradley, R. S., Vuille, M., Hardy, D., and Thompson, L. G.: Low latitude ice cores record Pacific sea surface temperatures, Geophysical Research Letters, 30, 2–5, https://doi.org/10.1029/2002GL016546, 2003.

Braun, L. N., Weber, M., and Schulz, M.: Consequences of climate change for runoff from Alpine regions, Annals of Glaciology, 31, 19–25, https://doi.org/10.3189/172756400781820165, 2000.

Bury, J., Mark, B. G., Carey, M., Young, K. R., McKenzie, J. M., Baraer, M., French, A., and Polk, M. H.: New Geographies of Water and Climate Change in Peru: Coupled Natural and Social Transformations in the Santa River Watershed, Annals of the Association of American Geographers, 103, 363–374, https://doi.org/10.1080/00045608.2013.754665, 2013.

Bury, J. T., Mark, B. G., McKenzie, J. M., French, A., Baraer, M., Huh, K. I., Zapata Luyo, M. A., and Gómez López, R. J.: Glacier recession and human vulnerability in the Yanamarey watershed of the Cordillera Blanca, Peru, Climatic Change, 105, 179–206, https://doi.org/10.1007/s10584-010-9870-1, 2011.

Buytaert, W. and Beven, K.: Models as multiple working hypotheses: hydrological simulation of tropical alpine wetlands, Hydrological Processes, 25, 1784–1799, https://doi.org/10.1002/hyp.7936, 2011.

Buytaert, W., Célleri, R., De Bièvre, B., Cisneros, F., Wyseure, G., Deckers, J., and Hofstede, R.: Human impact on the hydrology of the Andean páramos, Earth-Science Reviews, 79, 53–72, https://doi.org/10.1016/j.earscirev.2006.06.002, 2006.

Caceres, B., Francou, B., Favier, V., Bontron, G., Tachker, P., Bucher, R., Taupin, J.-D., Vuille, M., Maisincho, L., and Delachaux, F.: Glacier 15, Antisana, Ecuador: its glaciology and relations to water resources, 2006.

5 Carey, M., Molden, O. C., Rasmussen, M. B., Jackson, M., Nolin, A. W., and Mark, B. G.: Impacts of Glacier Recession and Declining Meltwater on Mountain Societies, Annals of the American Association of Geographers, 107, 350–359, https://doi.org/10.1080/24694452.2016.1243039, 2017.

Cauvy-Fraunié, S., Condom, T., Rabatel, A., Villacis, M., Jacobsen, D., and Dangles, O.: Technical Note: Glacial influence in tropical mountain hydrosystems evidenced by the diurnal cycle in water levels, Hydrology and Earth System Sciences, 17, 4803–4816,
10 https://doi.org/10.5194/hess-17-4803-2013, 2013.

Chen, J., Knight, R., and Zebker, H. A.: The Temporal and Spatial Variability of the Confined Aquifer Head and Storage Properties in the San Luis Valley, Colorado Inferred From Multiple InSAR Missions, Water Resources Research, 53, 9708–9720, https://doi.org/10.1002/2017WR020881, 2017.

Christophersen, N., Neal, C., Hooper, R. P., Vogt, R. D., and Andersen, S.: Modelling streamwater chemistry as a mixture of soilwater
15 end-members—a step towards second-generation acidification models, Journal of Hydrology, 116, 307–320, 1990.

Clapperton, C. M.: Glacial and volcanic geomorphology of the Chimborazo-Carihuairazo Massif, Ecuadorian Andes, Transactions of the Royal Society of Edinburgh: Earth Sciences, 81, 91–116, https://doi.org/10.1017/S0263593300005174, 1990.

Clow, D., Schrott, L., Webb, R., Campbell, D., Torizzo, A., and Dornblaser, M.: Ground Water Occurrence and Contributions to Streamflow in an Alpine Catchment, Colorado Front Range, Ground Water, 41, 937–950, https://doi.org/10.1111/j.1745-6584.2003.tb02436.x, 2003.

20 Crossman, J., Bradley, C., Boomer, I., and Milner, A. M.: Water Flow Dynamics of Groundwater-Fed Streams and Their Ecological Significance in a Glacierized Catchment, Arctic, Antarctic, and Alpine Research, 43, 364–379, https://doi.org/10.1657/1938-4246-43.3.364, 2011.

Ek, M. B., Mitchell, K. E., Lin, Y., Rogers, E., Grunmann, P., Koren, V., Gayno, G., and Tarpley, J. D.: Implementation of Noah land surface model advances in the National Centers for Environmental Prediction operational mesoscale Eta model, Journal of Geophysical Research:
25 Atmospheres, 108, 2003.

Engel, M., Penna, D., Bertoldi, G., Dell'Agnese, A., Soulsby, C., and Comiti, F.: Identifying run-off contributions during melt-induced run-off events in a glacierized alpine catchment, Hydrological Processes, 30, 343–364, https://doi.org/10.1002/hyp.10577, 2016.

Escher-Vetter, H., Reinwarth, O., and Rentsch, H.: Two decades of runoff measurements (1974 to 1993) at the pegelstation Vernagtbach/Oetztal alps, Zeitschrift für Gletscherkunde und Glazialgeologie, 30, 99–107, 1994.

30 Farr, T. G., Rosen, P. A., Caro, E., Crippen, R., Duren, R., Hensley, S., Kobrick, M., Paller, M., Rodriguez, E., and Roth, L.: The shuttle radar topography mission, Reviews of Geophysics, 45, 2007.

Favier, V.: Glaciers of the outer and inner tropics: A different behaviour but a common response to climatic forcing, Geophysical Research Letters, 31, L16 403, https://doi.org/10.1029/2004GL020654, 2004.

Favier, V., Coudrain, A., Cadier, E., Francou, B., Ayabaca, E., Maisincho, L., Praderio, E., Villacis, M., and Wagnon, P.: Evidence of
35 groundwater flow on Antizana ice-covered volcano, Ecuador / Mise en évidence d'écoulements souterrains sur le volcan englacé Antizana, Equateur, Hydrological Sciences Journal, 53, 278–291, https://doi.org/10.1623/hysj.53.1.278, 2008a.

Favier, V., Coudrain, A., Cadier, E., Francou, B., Ayabaca, E., MAISINCHO, L., Praderio, E., Villacis, M., and Wagnon, P.: Evidence of groundwater flow on Antizana ice-covered volcano, Ecuador / Mise en évidence d'écoulements souterrains sur le volcan englacé Antizana, Equateur, Hydrological Sciences Journal, 53, 278–291, https://doi.org/10.1623/hysj.53.1.278, 2008b.

Fernández, A. and Mark, B. G.: Modeling modern glacier response to climate changes along the Andes Cordillera: A multiscale review, Journal of Advances in Modeling Earth Systems, 8, 467–495, 2016.

Fountain, A. G. and Tangborn, W. V.: The Effect of Glaciers on Streamflow Variations, Water Resources Research, 21, 579–586, https://doi.org/10.1029/WR021i004p00579, 1985.

Francou, B.: Tropical climate change recorded by a glacier in the central Andes during the last decades of the twentieth century: Chacaltaya, Bolivia, 16S, Journal of Geophysical Research, 108, 4154, https://doi.org/10.1029/2002JD002959, 2003.

Francou, B.: New evidence for an ENSO impact on low-latitude glaciers: Antizana 15, Andes of Ecuador, Journal of Geophysical Research, 109, D18 106, https://doi.org/10.1029/2003JD004484, 2004.

Frenierre, J. L. and Mark, B. G.: A review of methods for estimating the contribution of glacial meltwater to total watershed discharge, Progress in Physical Geography, 38, 173–200, https://doi.org/10.1177/0309133313516161, 2014.

Frisbee, M. D., Phillips, F. M., Campbell, A. R., Liu, F., and Sanchez, S. A.: Streamflow generation in a large, alpine watershed in the southern Rocky Mountains of Colorado: Is streamflow generation simply the aggregation of hillslope runoff responses?, Water Resour. Res., 47, 1–18, https://doi.org/10.1029/2010WR009391, 2011.

Gabbi, J., Carenzo, M., Pellicciotti, F., Bauder, A., and Funk, M.: A comparison of empirical and physically based glacier surface melt models for long-term simulations of glacier response, Journal of Glaciology, 60, 1140–1154, https://doi.org/10.3189/2014JoG14J011, 2014.

Gordon, R. P., Lautz, L. K., McKenzie, J. M., Mark, B. G., Chavez, D., and Baraer, M.: Sources and pathways of stream generation in tropical proglacial valleys of the Cordillera Blanca, Peru, Journal of Hydrology, 522, 628–644, https://doi.org/10.1016/j.jhydrol.2015.01.013, 2015.

Harden, D. R.: California geology, Prentice Hall, 2004.

Harpold, A. A. and Brooks, P. D.: Humidity determines snowpack ablation under a warming climate, Proceedings of the National Academy of Sciences, 115, 1215–1220, https://doi.org/10.1073/pnas.1716789115, 2018.

Harrington, J. S., Mozil, A., Hayashi, M., and Bentley, L. R.: Groundwater flow and storage processes in an inactive rock glacier, Hydrol. Process., 32, 3070–3088, https://doi.org/10.1002/hyp.13248, 2018.

He, Z., Vorogushyn, S., Unger-Shayesteh, K., Gafurov, A., Kalashnikova, O., Omorova, E., and Merz, B.: The value of hydrograph partitioning curves for calibrating hydrological models in glacierized basins, Water Resources Research, pp. 1–52, https://doi.org/10.1002/2017WR021966, 2018.

Hock, R.: A distributed temperature-index ice- and snowrnelt model including potential direct solar radiation, Journal qf Glaciology, 45, 1999.

Hock, R.: Glacier melt: a review of processes and their modelling, Progress in physical geography, 29, 362–391, 2005.

Hood, J. L., Roy, J. W., and Hayashi, M.: Importance of groundwater in the water balance of an alpine headwater lake, Geophys. Res. Lett., 33, L13 405, https://doi.org/10.1029/2006GL026611, 2006.

Hooper, R. P.: Diagnostic tools for mixing models of stream water chemistry, Water Resources Research, 39, 2003.

Hooper, R. P. and Shoemaker, C. A.: A Comparison of Chemical and Isotopic Hydrograph Separation, Water Resources Research, 22, 1444–1454, https://doi.org/10.1029/WR022i010p01444, 1986.

Huss, M., Bauder, A., Funk, M., and Hock, R.: Determination of the seasonal mass balance of four Alpine glaciers since 1865, Journal of Geophysical Research, 113, F01 015, https://doi.org/10.1029/2007JF000803, 2008.

Huss, M., Funk, M., and Ohmura, A.: Strong Alpine glacier melt in the 1940s due to enhanced solar radiation, Geophysical Research Letters, 36, L23 501, https://doi.org/10.1029/2009GL040789, 2009.

5   Huth, A. K., Leydecker, A., Sickman, J. O., and Bales, R. C.: A two-component hydrograph separation for three high-elevation catchments in the Sierra Nevada, California, Hydrol. Process., 18, 1721–1733, https://doi.org/10.1002/hyp.1414, 2004.

Immerzeel, W. W., van Beek, L. P. H., and Bierkens, M. F. P.: Climate Change Will Affect the Asian Water Towers, Science, 328, 1382–1385, https://doi.org/10.1126/science.1183188, 2010.

INEC: Cencos de Poblacion y Vivienda 2010, Quito, Ecuador, 2010.

10   James, A. L. and Roulet, N. T.: Investigating the applicability of end-member mixing analysis (EMMA) across scale: A study of eight small, nested catchments in a temperate forested watershed, Water Resources Research, 42, 2006.

Jansson, P., Hock, R., and Schneider, T.: The concept of glacier storage: a review, Journal of Hydrology, 282, 116–129, https://doi.org/10.1016/S0022-1694(03)00258-0, 2003.

Jasechko, S., Kirchner, J. W., Welker, J. M., and McDonnell, J. J.: Substantial proportion of global streamflow less than three months old,
15   Nature Geoscience, 9, 126–129, https://doi.org/10.1038/ngeo2636, 2016.

Jordan, E., González, J., Castillo, K., Torres, J., Ungerechts, L., Vélez, F., Blanco, D., and Cruz, M.: Ortofotomapa del Chimborazo y su valor como diagnóstico para cambios climaticos en relacion con otros glaciares tropicales [Orthophotomap of Chimborazo and its value as a diagnosis for climatic changes in relation to other tropical glaciers], Glaciares, Nieves y Hielos de America Latina: Cambio Climatico y Amenazas, pp. 239–260, 2010.

20   Juen, I., Kaser, G., and Georges, C.: Modelling observed and future runoff from a glacierized tropical catchment (Cordillera Blanca, Perú), Global and Planetary Change, 59, 37–48, https://doi.org/10.1016/j.gloplacha.2006.11.038, 2007.

Kaser, G.: A review of the modern fluctuations of tropical glaciers, Global and Planetary Change, 22, 93–103, https://doi.org/10.1016/S0921-8181(99)00028-4, 1999.

Kaser, G. and Osmaston, H.: Tropical glaciers, Cambridge University Press, 2002.

25   Kendall, C., Doctor, D., Drever, J., Holland, H., and Turekian, K.: Stable isotope applications in hydrological studies, pp. 319–364, https://doi.org/http://dx.doi.org/10.1016/B0-08-043751-6/05081-7, 2003.

La Frenierre, J.: Rapid downward deflation of a tropical-debris covered glacier: an analysis from Volcán Chimborazo, Ecuador, in: AGU Fall Meeting Abstracts, 2016.

La Frenierre, J. and Mark, B. G.: Detecting Patterns of Climate Change at Volcán Chimborazo, Ecuador, by Integrating Instrumen-
30   tal Data, Public Observations, and Glacier Change Analysis, Annals of the American Association of Geographers, 107, 979–997, https://doi.org/10.1080/24694452.2016.1270185, 2017.

La Frenierre, J. D.: Assessing the Hydrologic Implications of Glacier Recession and the Potential for Water Resources Vulnerability at Volcán Chimborazo, Ecuador, p. 255, 2014.

Lang, H.: Forecasting Meltwater Runoff from Snow-Covered Areas and from Glacier Basins, pp. 99–127, Springer Netherlands, Dordrecht,
35   https://doi.org/10.1007/978-94-009-4536-4_5, 1986.

Liu, F., Williams, M. W., and Caine, N.: Source waters and flow paths in an alpine catchment, Colorado Front Range, United States, Water Resources Research, 40, 1–16, https://doi.org/10.1029/2004WR003076, 2004.

Loheide, S. P., Deitchman, R. S., Cooper, D. J., Wolf, E. C., Hammersmark, C. T., and Lundquist, J. D.: A framework for understanding the hydroecology of impacted wet meadows in the Sierra Nevada and Cascade Ranges, California, USA, Hydrogeology Journal, 17, 229–246, https://doi.org/10.1007/s10040-008-0380-4, 2009.

5   Lowry, C. S., Deems, J. S., Loheide II, S. P., and Lundquist, J. D.: Linking snowmelt-derived fluxes and groundwater flow in a high elevation meadow system, Sierra Nevada Mountains, California, Hydrological Processes, 24, 2821–2833, https://doi.org/10.1002/hyp.7714, 2010.

Lowry, C. S., Loheide, S. P., Moore, C. E., and Lundquist, J. D.: Groundwater controls on vegetation composition and patterning in mountain meadows, Water Resources Research, 47, 1–16, https://doi.org/10.1029/2010WR010086, 2011.

Luce, C. H.: Effects of Climate Change on Snowpack, Glaciers, and Water Resources in the Northern Rockies, pp. 25–36, Springer International Publishing, Cham, https://doi.org/10.1007/978-3-319-56928-4_3, 2018.

10   Mackay, A.: Climate Change 2007: Impacts, Adaptation and Vulnerability. Contribution of Working Group II to the Fourth Assessment Report of the Intergovernmental Panel on Climate Change, Journal of Environment Quality, 37, 2407, https://doi.org/10.2134/jeq2008.0015br, 2008.

Manciati, C., Villacís, M., Taupin, J.-D., Cadier, E., Galárraga-Sánchez, R., and Cáceres, B.: Empirical mass balance modelling of South American tropical glaciers: case study of Antisana volcano, Ecuador, Hydrological Sciences Journal, 59, 1519–1535,
15   https://doi.org/10.1080/02626667.2014.888490, 2014.

Mark, B. G.: Tracing tropical Andean glaciers over space and time: Some lessons and transdisciplinary implications, Global and Planetary Change, 60, 101–114, https://doi.org/10.1016/j.gloplacha.2006.07.032, 2008.

Mark, B. G. and Mckenzie, J. M.: Tracing Increasing Tropical Andean Glacier Melt with Stable Isotopes in Water, Environmental Science & Technology, 41, 6955–6960, https://doi.org/10.1021/es071099d, 2007.

20   Mark, B. G. and Seltzer, G. O.: Tropical glacier meltwater contribution to stream discharge: a case study in the Cordillera Blanca, Peru, Journal of Glaciology, 49, 271–281, https://doi.org/10.3189/172756503781830746, 2003.

Mark, B. G., McKenzie, J. M., and Gómez, J.: Hydrochemical evaluation of changing glacier meltwater contribution to stream discharge: Callejon de Huaylas, Peru / Evaluation hydrochimique de la contribution évolutive de la fonte glaciaire à l'écoulement fluvial: Callejon de Huaylas, Pérou, Hydrological Sciences Journal, 50, 975–988, https://doi.org/10.1623/hysj.2005.50.6.975, 2005.

25   Markovich, K. H., Maxwell, R. M., and Fogg, G. E.: Hydrogeological response to climate change in alpine hillslopes, Hydrological Processes, 30, 3126–3138, https://doi.org/10.1002/hyp.10851, 2016.

Maussion, F., Gurgiser, W., Großhauser, M., Kaser, G., and Marzeion, B.: ENSO influence on surface energy and mass balance at Shallap Glacier, Cordillera Blanca, Peru, The Cryosphere, 9, 1663–1683, 2015.

McLaughlin, R.: Hydrochemical Signatures of Glacial Meltwater on Volcán Chimborazo, Ecuador, Ph.D. thesis, 2017.

30   Messerli, B., Viviroli, D., and Weingartner, R.: Mountains of the World: Vulnerable Water Towers for the 21st Century, AMBIO Special Report, 13, 29–34, https://doi.org/10.5167/uzh-110516, 2004.

Minaya, Maldonado, V. G.: Ecohydrology of the Andes Páramo Region, PhD diss., IHE Delft Institute for Water Education, 2016.

Ng, G.-H. C., Wickert, A. D., Somers, L. D., Saberi, L., Cronkite-Ratcliff, C., Niswonger, R. G., and McKenzie, J. M.: GSFLOW-GRASS v1. 0.0: GIS-enabled hydrologic modeling of coupled groundwater–surface-water systems, Manuscript under review for journal Geosci.
35   Model Dev., 2018.

NRCS, U.: Part 630 Hydrology National Engineering Handbook, 2009.

Omani, N., Srinivasan, R., Smith, P. K., and Karthikeyan, R.: Glacier mass balance simulation using SWAT distributed snow algorithm, Hydrological Sciences Journal, 62, 546–560, https://doi.org/10.1080/02626667.2016.1162907, 2017.

Ostheimer, G. J., Hadjivasiliou, H., Kloer, D. P., Barkan, A., and Matthews, B. W.: Structural Analysis of the Group II Intron Splicing Factor CRS2 Yields Insights into its Protein and RNA Interaction Surfaces, Journal of Molecular Biology, 345, 51–68, https://doi.org/10.1016/j.jmb.2004.10.032, 2005.

Pellicciotti, F., Brock, B., Strasser, U., Burlando, P., Funk, M., and Corripio, J.: An enhanced temperature-index glacier melt model including the shortwave radiation balance: development and testing for Haut Glacier d'Arolla, Switzerland, Journal of Glaciology, 51, 573–587, 2005.

Pepin, N., Bradley, R. S., Diaz, H. F., Baraer, M., Caceres, E. B., Forsythe, N., Fowler, H., Greenwood, G., Hashmi, M. Z., Liu, X. D., Miller, J. R., Ning, L., Ohmura, A., Palazzi, E., Rangwala, I., Schöner, W., Severskiy, I., Shahgedanova, M., Wang, M. B., Williamson, S. N., and Yang, D. Q.: Elevation-dependent warming in mountain regions of the world, Nature Climate Change, 5, 424–430, https://doi.org/10.1038/nclimate2563, 2015.

Podwojewski, P., Poulenard, J., Zambrana, T., and Hofstede, R.: Overgrazing effects on vegetation cover and properties of volcanic ash soil in the pàramo of Llangahua and al Esperanza (Tungurahua, Ecuador), Management, 18, 45–55, https://doi.org/10.1079/SUM2001100, 2002.

Pohl, E., Knoche, M., Gloaguen, R., Andermann, C., and Krause, P.: Sensitivity analysis and implications for surface processes from a hydrological modelling approach in the Gunt catchment, high Pamir Mountains, Earth Surf. Dyn., 3, 333–362, https://doi.org/10.5194/esurf-3-333-2015, 2015.

Polk, M. H., Young, K. R., Baraer, M., Mark, B. G., McKenzie, J. M., Bury, J., and Carey, M.: Exploring hydrologic connections between tropical mountain wetlands and glacier recession in Peru's Cordillera Blanca, Applied Geography, 78, 94–103, https://doi.org/10.1016/j.apgeog.2016.11.004, 2017.

Pribulick, C. E., Foster, L. M., Bearup, L. A., Navarre-Sitchler, A. K., Williams, K. H., Carroll, R. W., and Maxwell, R. M.: Contrasting the hydrologic response due to land cover and climate change in a mountain headwaters system, Ecohydrology, 9, 1431–1438, https://doi.org/10.1002/eco.1779, 2016.

Qu, Y. and Duffy, C. J.: A semidiscrete finite volume formulation for multiprocess watershed simulation, Water Resources Research, 43, 1–18, https://doi.org/10.1029/2006WR005752, 2007.

Rabatel, A., Francou, B., Soruco, A., Gomez, J., Cáceres, B., Ceballos, J. L., Basantes, R., Vuille, M., Sicart, J.-E., Huggel, C., Scheel, M., Lejeune, Y., Arnaud, Y., Collet, M., Condom, T., Consoli, G., Favier, V., Jomelli, V., Galarraga, R., Ginot, P., Maisincho, L., Mendoza, J., Ménégoz, M., Ramirez, E., Ribstein, P., Suarez, W., Villacis, M., and Wagnon, P.: Current state of glaciers in the tropical Andes: a multi-century perspective on glacier evolution and climate change, The Cryosphere, 7, 81–102, https://doi.org/10.5194/tc-7-81-2013, 2013.

Reveillet, M., Vincent, C., Six, D., and Rabatel, A.: Which empirical model is best suited to simulate glacier mass balances?, Journal of Glaciology, 63, 39–54, https://doi.org/10.1017/jog.2016.110, 2017.

Rodell, M., Houser, P. R., Jambor, U. E. A., Gottschalck, J., Mitchell, K., Meng, C. J., Arsenault, K., Cosgrove, B., Radakovich, J., and Bosilovich, M.: The global land data assimilation system, Bulletin of the American Meteorological Society, 85, 381–394, 2004.

Ryu, J.-S., Lee, K.-S., and Chang, H.-W.: Hydrochemistry and isotope geochemistry of Song Stream, a headwater tributary of the South Han River, South Korea, Geosciences Journal, 11, 157–164, https://doi.org/10.1007/BF02913929, 2007.

Samaniego, P., Barba, D., Robin, C., Fornari, M., and Bernard, B.: Eruptive history of Chimborazo volcano (Ecuador): A large, ice-capped and hazardous compound volcano in the Northern Andes, Journal of Volcanology and Geothermal Research, 221-222, 33–51, https://doi.org/10.1016/j.jvolgeores.2012.01.014, 2012.

Sarmiento, L.: Water Balance and Soil Loss under Long Fallow Agriculture in the Venezuelan Andes, Mountain Research and Development, 20, 246–253, 2000.

Schmieder, J., Garvelmann, J., Marke, T., and Strasser, U.: Spatio-temporal tracer variability in the glacier melt end-member - How does it affect hydrograph separation results?, Hydrological Processes, 2016, https://doi.org/10.1002/hyp.11628, 2018.

5   Shi, Y., Davis, K. J., Duffy, C. J., and Yu, X.: Development of a Coupled Land Surface Hydrologic Model and Evaluation at a Critical Zone Observatory, Journal of Hydrometeorology, 14, 1401–1420, https://doi.org/10.1175/JHM-D-12-0145.1, 2013.

Sicart, J. E., Hock, R., and Six, D.: Glacier melt, air temperature, and energy balance in different climates: The Bolivian Tropics, the French Alps, and northern Sweden, Journal of Geophysical Research, 113, D24 113, https://doi.org/10.1029/2008JD010406, 2008.

Smith, J. A., Mark, B. G., and Rodbell, D. T.: The timing and magnitude of mountain glaciation in the tropical Andes, Journal of Quaternary

10   Science, 23, 609–634, https://doi.org/10.1002/jqs.1224, 2008.

Somers, L. D., Gordon, R. P., McKenzie, J. M., Lautz, L. K., Wigmore, O., Glose, A. M., Glas, R., Aubry-Wake, C., Mark, B., Baraer, M., and Condom, T.: Quantifying groundwater-surface water interactions in a proglacial valley, Cordillera Blanca, Peru, Hydrological Processes, 30, 2915–2929, https://doi.org/10.1002/hyp.10912, 2016.

Soruco, A., Vincent, C., Rabatel, A., Francou, B., Thibert, E., Sicart, J. E., and Condom, T.: Contribution of glacier runoff to water resources

15   of La Paz city, Bolivia (16° S), Annals of Glaciology, 56, 147–154, https://doi.org/10.3189/2015AoG70A001, 2015.

Soulsby, C., Petry, J., Brewer, M., Dunn, S., Ott, B., and Malcolm, I.: Identifying and assessing uncertainty in hydrological pathways: a novel approach to end member mixing in a Scottish agricultural catchment, Journal of Hydrology, 274, 109–128, https://doi.org/10.1016/S0022-1694(02)00398-0, 2003.

Staudinger, M., Stoelzle, M., Seeger, S., Seibert, J., Weiler, M., and Stahl, K.: Catchment water storage variation with elevation, Hydrological

20   Processes, 31, 2000–2015, https://doi.org/10.1002/hyp.11158, 2017.

Suecker, J. K., Ryan, J. N., Kendall, C., and Jarrett, R. D.: Determination of hydrologic pathways during snowmelt for alpine/subalpine basins, Rocky Mountain National Park, Colorado, Water Resources Research, 36, 63–75, https://doi.org/10.1029/1999WR900296, 2000.

Tague, C. and Grant, G. E.: Groundwater dynamics mediate low-flow response to global warming in snow-dominated alpine regions, Water Resources Research, 45, 1–12, https://doi.org/10.1029/2008WR007179, 2009.

25   Tague, C., Grant, G., Farrell, M., Choate, J., and Jefferson, A.: Deep groundwater mediates streamflow response to climate warming in the Oregon Cascades, Climatic Change, 86, 189–210, https://doi.org/10.1007/s10584-007-9294-8, 2008.

Veettil, B. K., Leandro Bayer Maier, E., Bremer, U. F., and de Souza, S. F.: Combined influence of PDO and ENSO on northern Andean glaciers: a case study on the Cotopaxi ice-covered volcano, Ecuador, Climate Dynamics, 43, 3439–3448, https://doi.org/10.1007/s00382-014-2114-8, 2014a.

30   Veettil, B. K., Maier, E. L. B., Bremer, U. F., and de Souza, S. F.: Combined influence of PDO and ENSO on northern Andean glaciers: a case study on the Cotopaxi ice-covered volcano, Ecuador, Climate dynamics, 43, 3439–3448, 2014b.

Veettil, B. K., Bremer, U. F., de Souza, S. F., Maier, E. L. B., and Simões, J. C.: Influence of ENSO and PDO on mountain glaciers in the outer tropics: case studies in Bolivia, Theoretical and Applied Climatology, 125, 757–768, https://doi.org/10.1007/s00704-015-1545-4, 2016.

35   Vermote, E.: MOD09A1 MODIS/Terra Surface Reflectance 8-Day L3 Global 500m SIN Grid V006, NASA EOSDIS Land Processes DAAC, 2015.

Vuille, M. and Bradley, R. S.: the tropical Andes, Geophysical Research Letters, 27, 3885–3888, 2000.

Vuille, M. and Keimig, F.: Interannual Variability of Summertime Convective Cloudiness and Precipitation in the Central Andes Derived from ISCCP-B3 Data, Journal of Climate, 17, 3334–3348, https://doi.org/10.1175/1520-0442(2004)017<3334:IVOSCC>2.0.CO;2, 2004.

Vuille, M., Bradley, R. S., Werner, M., and Keimig, F.: 20th Century Climate Change in the Tropical Andes: Observations and Model Results, in: Climatic Change, vol. 59, pp. 75–99, https://doi.org/10.1007/978-94-015-1252-7_5, 2003.

5 Vuille, M., Francou, B., Wagnon, P., Juen, I., Kaser, G., Mark, B. G., and Bradley, R. S.: Climate change and tropical Andean glaciers: Past, present and future, Earth-Science Reviews, 89, 79–96, https://doi.org/10.1016/j.earscirev.2008.04.002, 2008.

Vuille, M., Carey, M., Huggel, C., Buytaert, W., Rabatel, A., Jacobsen, D., Soruco, A., Villacis, M., Yarleque, C., Elison Timm, O., Condom, T., Salzmann, N., and Sicart, J.-E.: Rapid decline of snow and ice in the tropical Andes – Impacts, uncertainties and challenges ahead, Earth-Science Reviews, 176, 195–213, https://doi.org/10.1016/j.earscirev.2017.09.019, 2018.

10 Wagnon, P., Ribstein, P., Francou, B., and Sicart, J. E.: Anomalous heat and mass budget of Glaciar Zongo , Bolivia , during the 1997 / 98 El Ni · o year, Journal of Glaciology, 47, 21–28, 2001.

Wang, X., Sun, L., Zhang, Y., and Luo, Y.: Rationalization of Altitudinal Precipitation Profiles in a Data-Scarce Glacierized Watershed Simulation in the Karakoram, Water, 8, 186, https://doi.org/10.3390/w8050186, 2016.

Wickert, A. D.: The ALog: Inexpensive, Open-Source, Automated Data Collection in the Field, The Bulletin of the Ecological Society of 15 America, 95, 166–176, 2014.

Wilson, A. M., Williams, M. W., Kayastha, R. B., and Racoviteanu, A.: Use of a hydrologic mixing model to examine the roles of meltwater, precipitation and groundwater in the Langtang River basin, Nepal, Annals of Glaciology, 57, 155–168, https://doi.org/10.3189/2016AoG71A067, 2016.

Wosten, J. H. M., Lilly, A., Nemes, A., and Le Bas, C.: Development and use of a database of hydraulic properties of European soils, 20 Geoderma, 90, 169–185, 1999.

Multi-scale temporal variability in meltwater contributions in a tropical glacierized watershed
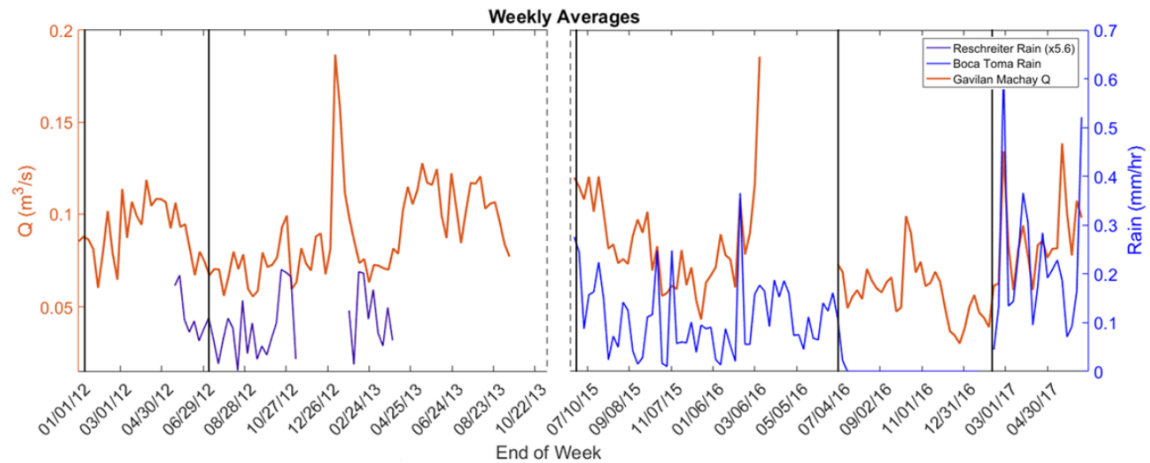
Figures

Figure S1. Comparison of average weekly discharge (m^3/s) at Gavilan Machay and rainfall (mm/hr) at Boca Toma. Vertical black dashed lines indicate weeks where sampling occurred. Despite gaps in data, it can be seen that precipitation was higher in the time surrounding the 2015 sampling campaign than in the times surrounding the other campaigns.
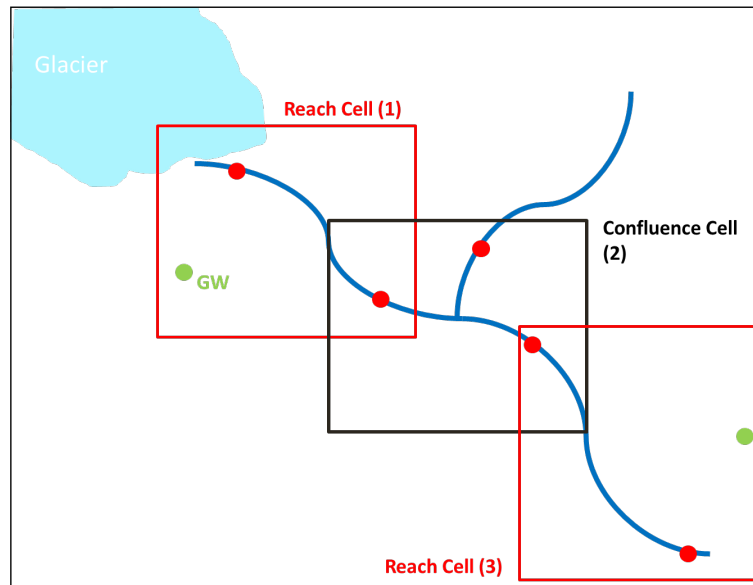

Figure S2. The reach and confluences cells relative to a stream system.
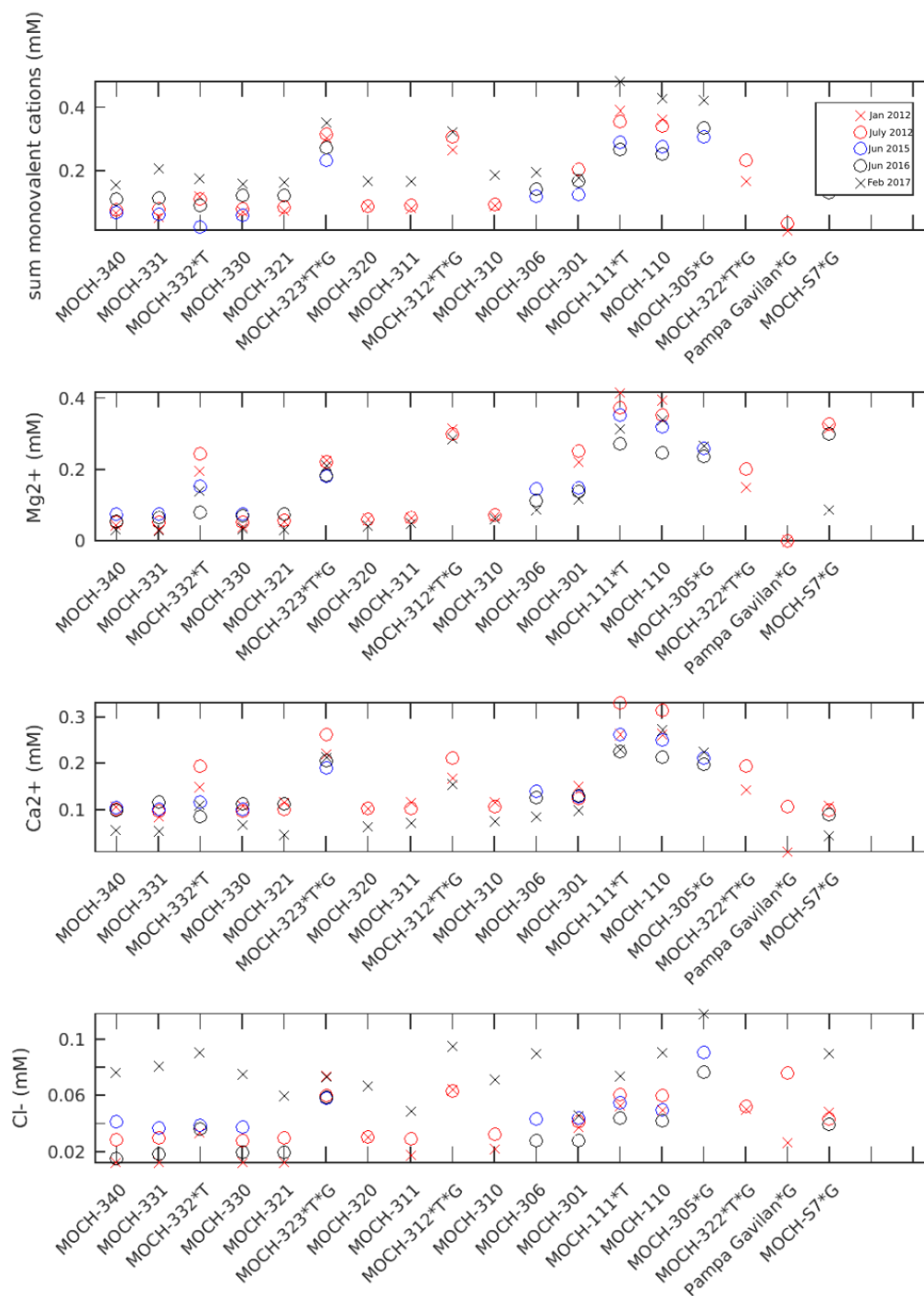
Figure S3. The concentrations of anions and cations across the different sampling periods.
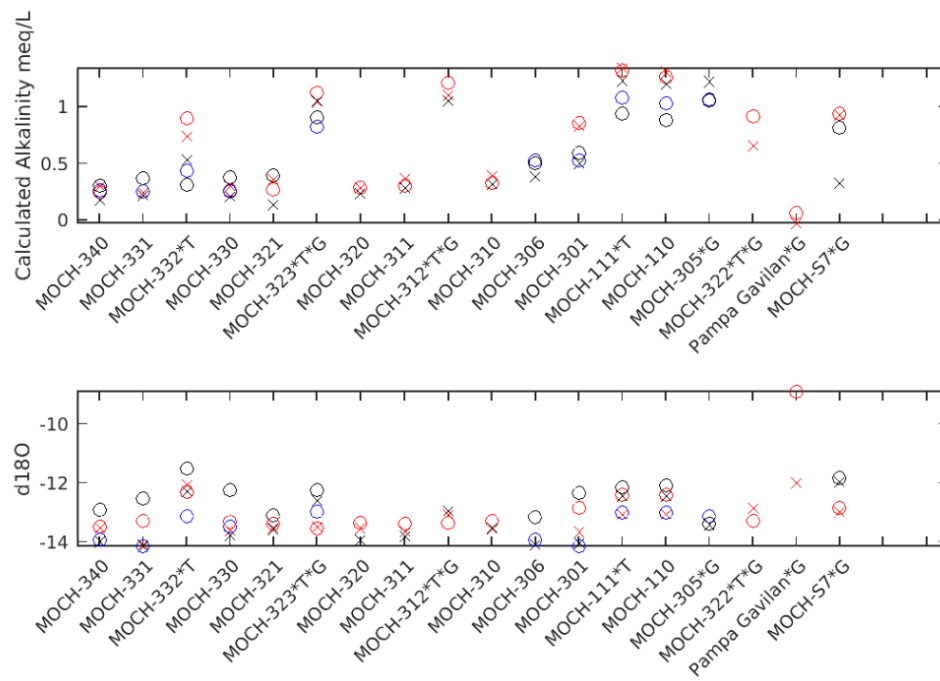
Figure S3. The concentrations of anions and cations across the different sampling periods.
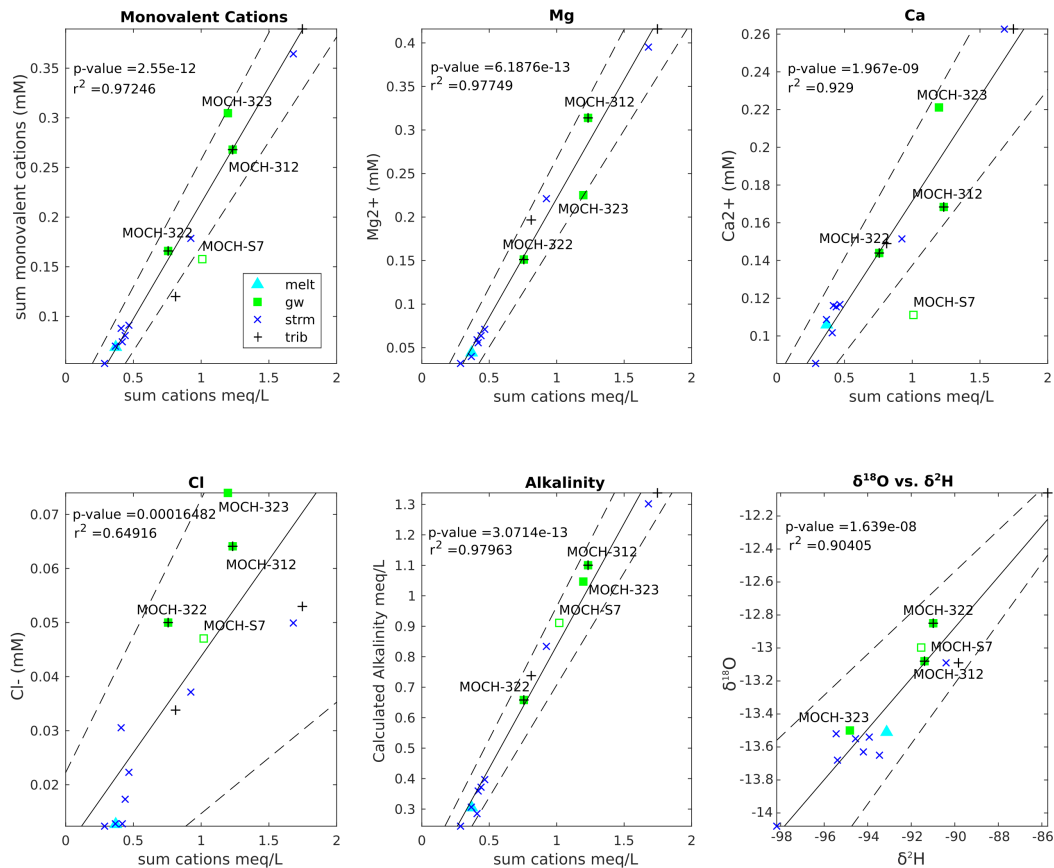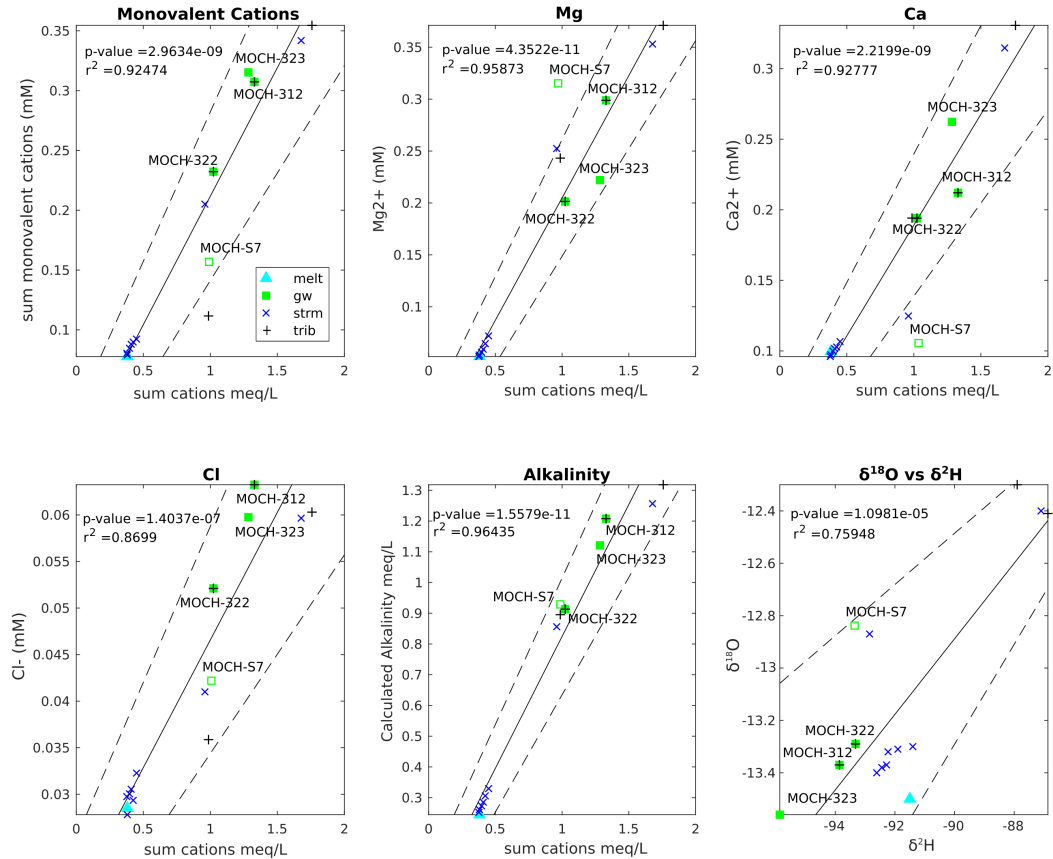
Figure S4. Bivariate diagrams of tracers selected for January 2012 analysis. The solid black lines represent linear regressions through all samples and dashed black lines indicated the regressions' 95% confidence intervals. Samples from the main Rio Mocha channel before and after the Gavilan stream joins it (filled green circles) consistently plot outside or away from the mixing line created between groundwater and meltwater. MOCH-S7 was not considered in the analysis (shown with hallow square). These samples are also responsible for the poor R2 and p-values of sulfate and chloride.
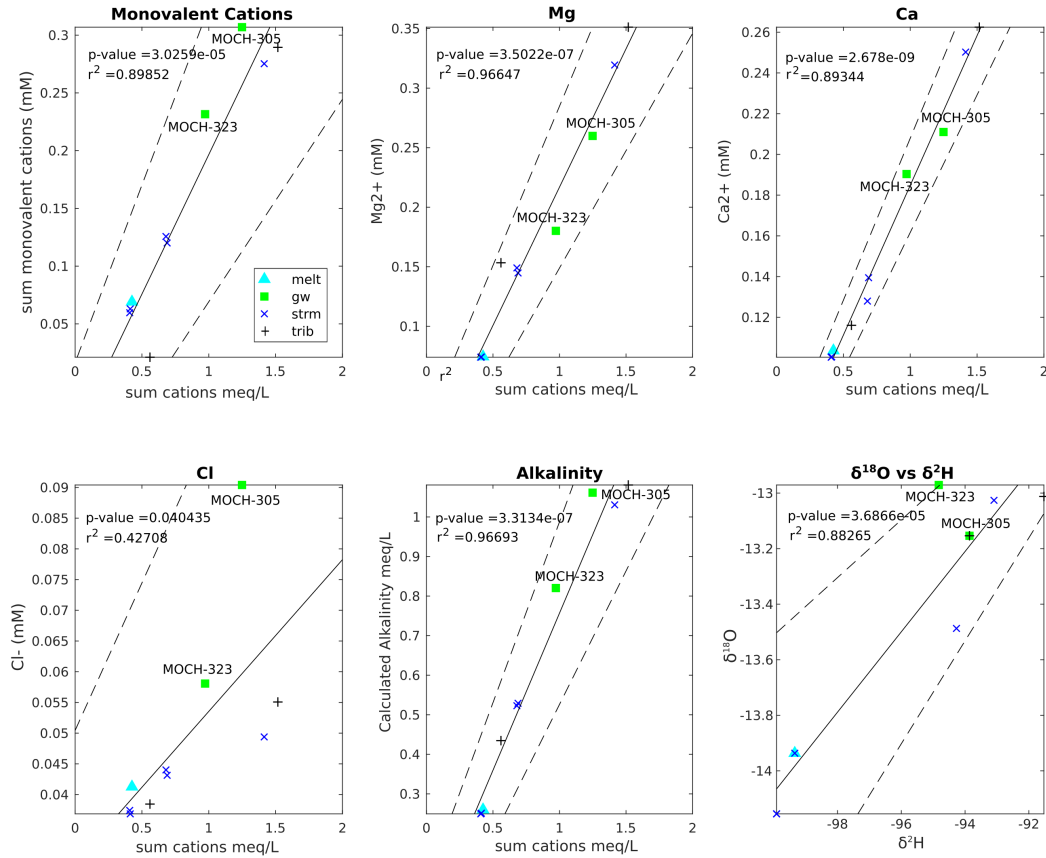
July 2012

Figure S5. Bivariate diagrams of tracers selected for July 2012 analysis. The solid black lines represent linear regressions through all samples and dashed black lines indicated the regressions' 95% confidence intervals. Samples from the main Rio Mocha channel before and after the Gavilan stream joins it (filled green circles) consistently plot outside or away from the mixing line created between groundwater and meltwater. MOCH-S7 was not considered in the analysis (shown with hollow square). These samples are also responsible for the poor R2 and p-values of sulfate and chloride.
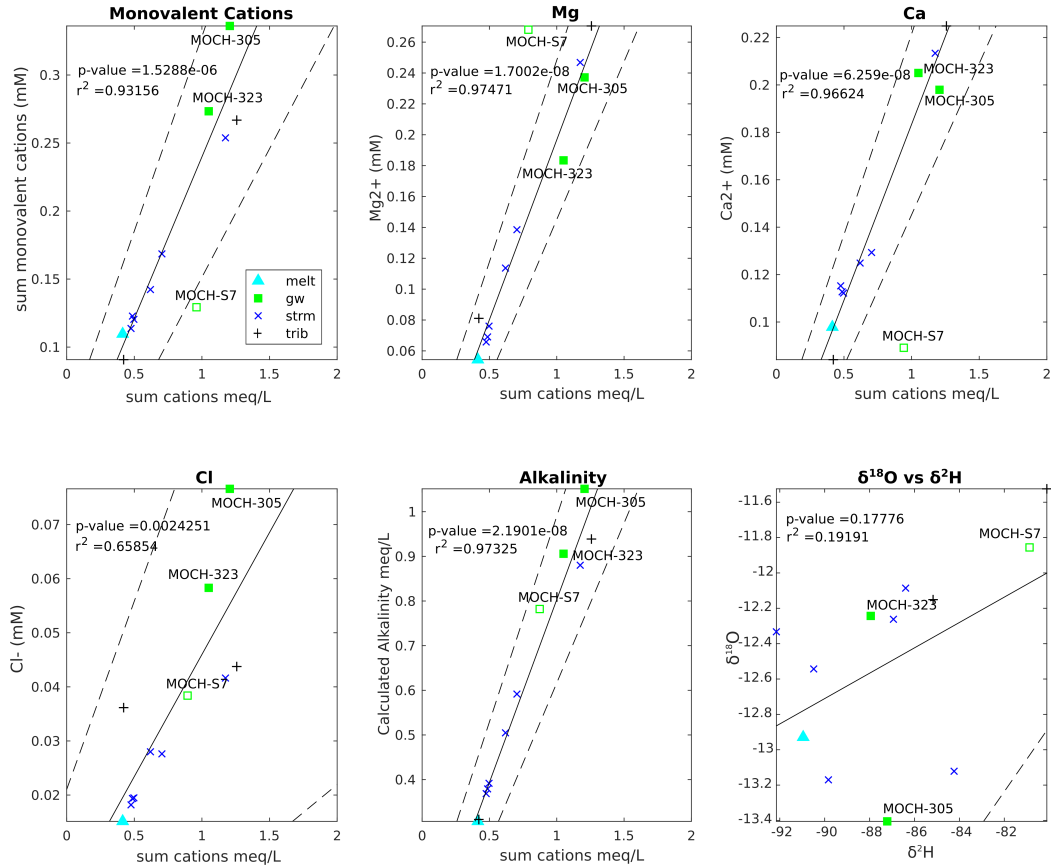
June 2015

Figure S6. Bivariate diagrams of tracers selected for June 2015 analysis. The solid black lines represent linear regressions through all samples and dashed black lines indicated the regressions' 95% confidence intervals. Samples from the main Rio Mocha channel before and after the Gavilan stream joins it (filled green circles) consistently plot outside or away from the mixing line created between groundwater and meltwater. MOCH-S7 was not considered in the analysis (shown with hallow square). These samples are also responsible for the poor R2 and p-values of sulfate and chloride.

June 2016

Figure S7. Bivariate diagrams of tracers selected for June 2016 analysis. The solid black lines represent linear regressions through all samples and dashed black lines indicated the regressions' 95% confidence intervals. Samples from the main Rio Mocha channel before and after the Gavilan stream joins it (filled green circles) consistently plot outside or away from the mixing line created between groundwater and meltwater. MOCH-S7 was not considered in the analysis (shown with hallow square). These samples are also responsible for the poor R2 and p-values of sulfate and chloride.
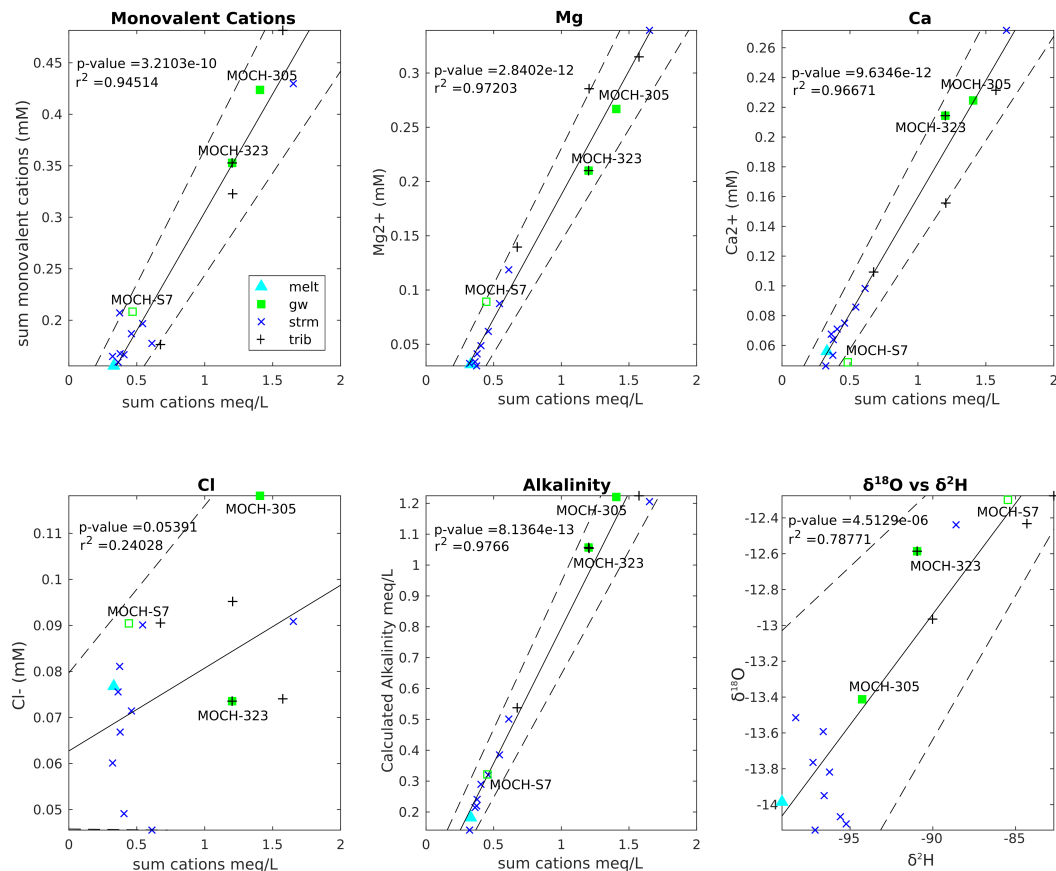
7

Figure S8. Bivariate diagrams of tracers selected for February 2017 analysis. The solid black lines represent linear regressions through all samples and dashed black lines indicated the regressions' 95% confidence intervals. Samples from the main Rio Mocha channel before and after the Gavilan stream joins it (filled green circles) consistently plot outside or away from the mixing line created between groundwater and meltwater. MOCH-S7 was not considered in the analysis (shown with hallow square). These samples are also responsible for the poor R2 and p-values of sulfate and chloride.
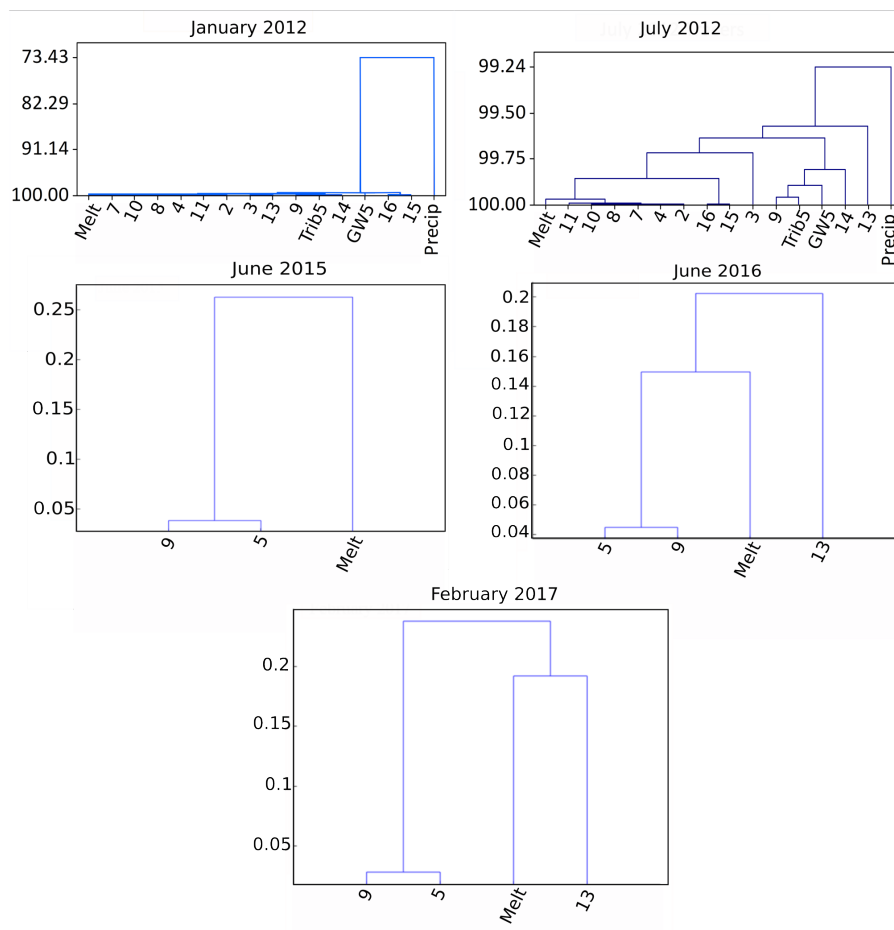
Figure S9. Hierarchical cluster analysis dendrograms for tracers used in HCBM for January 2012, July 2012, June 2015, June 2016, and February 2017. Sample grouping verifies effectiveness of selected tracers in distinguishing between source waters, as groundwater samples (GW) cluster separately from melt water (Melt) samples. GW-7 is considered an outlier, and is suspected to be a mixed source sample or to originate from a unique geology.
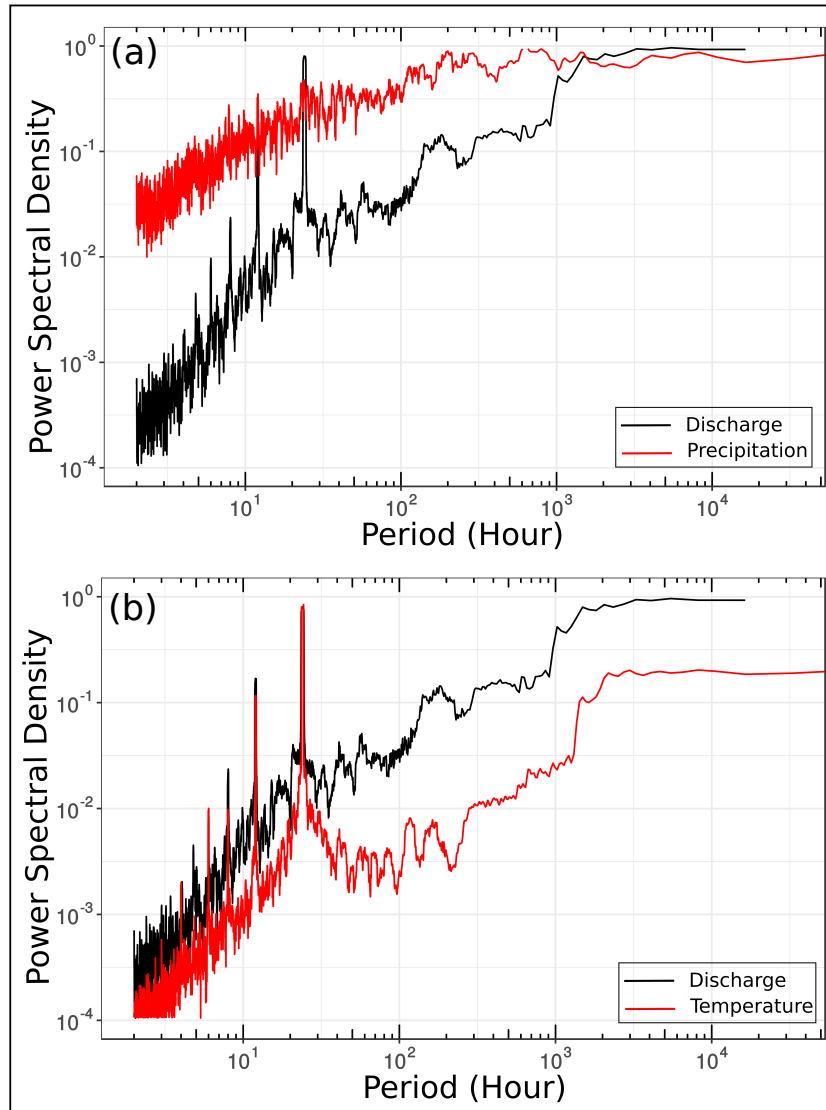
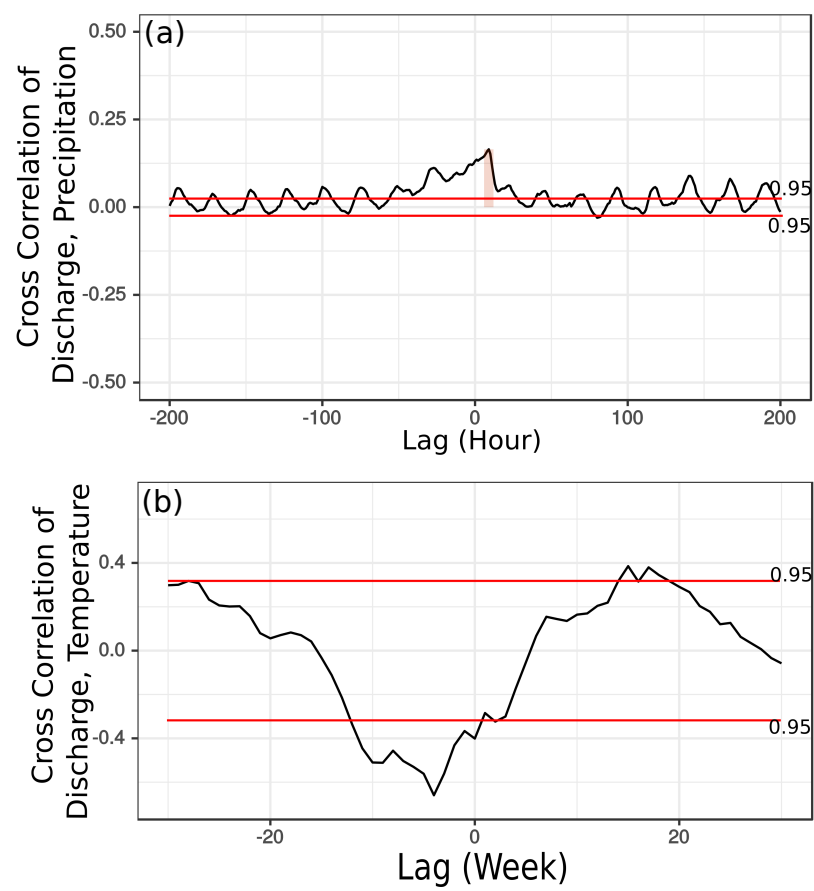**Figure S10.** Power spectral density of **(a)**discharge and temperature, **(b)** discharge and precipitation

Figure S11. Cross-correlation of **(a)**hourly discharge and precipitation, **(b)** weekly discharge and temperature
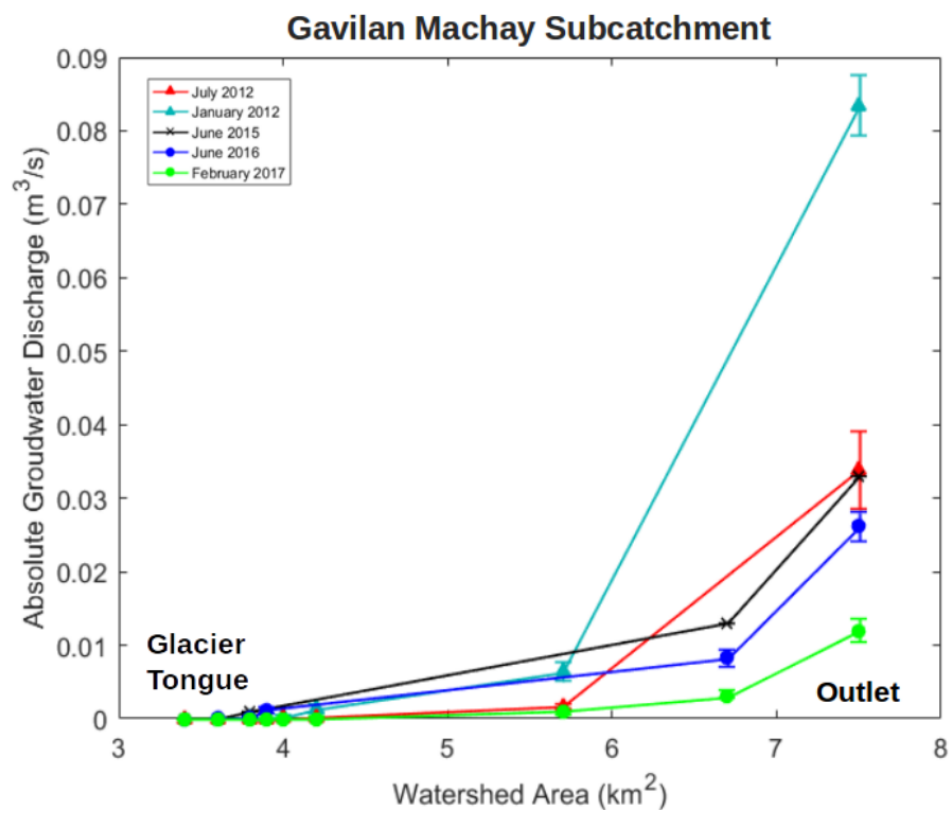
Figure S12. Calculated absolute groundwater discharge versus percentage of total watershed area drained for Gavilan Machay subcatchment (McLaughlin, 2017).

Hydrochemical Basin Characterization Model (HBCM)

The following set of mass-balance equations for J tracers applies to each HBCM cell:

$$C_{tot_j} = \frac{\sum_{i=1}^{I}(C_{i,j} * Q_i) + \epsilon_j}{Q_{tot}} \tag{S1}$$

Where:

j: index for a specific natural tracer, 1 through J

i: index for a specific source to the cell (ice, tributary, or groundwater), 1 through I

C_{tot_j}: concentration of tracer j at the cell outlet

$C_{i,j}$: concentration of tracer j in source i

Q_{tot}: Total discharge at cell outlet

Q_i: Contribution to discharge from source i

ϵ_j: residual error between the observed and predicted concentration flux out of the cell for tracer j

HBCM solves for the unknown relative contributions of each source (Q_i/Q_{tot}) by minimizing the sum of the residual errors:

$$\sum_{j=1}^{J} \epsilon_j \tag{S2}$$

In order to over-constrain the problem, the model requires $J = I$ tracers and, preferably, $J > I$ tracers should be utilized in order to avoid the possibility of correlated tracers that do not independently constrain the problem. HBCM checks that a tracer is conservative within each cell via three tests:

1. A tracer value in a cell outflow cannot be outside the range bracketed by the possible contributors;

2. The tracer value at the cell outflow, along with that of at least one input component, must be greater than the detection limit of the analytical methods (confirmed by user); and

3. There must be a minimum 5% difference between the concentration of a tracer from each source.

If any of these requirements is not met, HBCM will reject the tracer for use in the cell.

Tables

Table S1. HBCM analysis result for January 2012 to February 2017 with different cell configurations. – See the spreadsheet "HBCM Table".

	Observed				Flux-PIHM pedotransfer function results						
	Sand (%mass)	Silt (%mass)	Clay (%mass)	OC (%mass)	KINF (m/s)	KSATV (m/s)	KSATH (m/s)	SMCMAX (-)	SMCMIN (-)	ALPHA (1/m)	BETA (-)
Podwojewski et al. 2002, Pantano 60-80	26	41	8	12	4.52E-07	6.44E-07	6.44E-06	0.479	0.05	1.908	1.157
Patano 80-95+	33	39	14	8	1.47E-06	1.58E-06	1.58E-05	0.481	0.05	3.491	1.136
Humid páramo 0-15	26	44	7	10	6.24E-07	1.03E-06	1.03E-05	0.48	0.05	2.267	1.173
Humid páramo 15-30	32	41	8	7	1.51E-05	6.76E-06	3.05E-05	0.418	0.05	5.34	1.26
Dry páramo 0-15	30	43	8	7	8.28E-05	3.71E-05	6.96E-05	0.493	0.05	5.82	1.22
Dry páramo 15-30	35	33	20	5	8.28E-05	3.71E-05	6.96E-05	0.493	0.05	5.82	1.22
Minaya (2016), Low Elev.	20.28	31.98	6.24	22	3.71E-08	8.42E-08	8.42E-07	0.482	0.05	0.327	1.144
Minaya (2016), Middle Elev.	26.07	30.81	11.06	21	6.13E-08	1.03E-07	1.03E-06	0.479	0.05	0.466	1.124
Minaya (2016), Highest Elev.	23.4	39.6	6.3	10	4.28E-07	1.70E-07	1.70E-06	0.465	0.05	1.442	1.1

Table S2. Páramo soil measurments applied into pedo transfer functions (Podwojewski et al., 2002; Minaya, 2016)